Pergamon

Progress in Nuclear Energy, Vol. 31, No. 1/2, pp. 83–110, 1997

Printed in Great Britain
0149-1970/97 $32.00

PII: S0149-1970(96)00005-4

METALLIC FAST REACTOR FUELS*

G. L. HOFMAN, L. C. WALTERS, and T. H. BAUER

Argonne National Laboratory
Argonne, IL 60439

ABSTRACT

Metallic fuels are neutronically ideal for fast reactors because they produce an extremely hard neutron spectrum. Early metallic fuels had little endurance, due to excessive swelling. By incorporating space for swelling, very high burnups are now routinely achieved. Uranium-plutonium alloys with 10% zirconium to raise the melting point have been shown to be extremely reliable. Fuel swelling, mechanical and chemical interactions with various cladding materials, performance during transients, failure mechanisms, and behavior following both benign and complete failure of fuel pins have been extensively studied. The basic phenomena governing the performance of this type of fuel are well known, and have been sufficiently well modeled to specify design parameters that will assure reliable performance.

KEYWORDS

EBR-II; electrorefining; fast reactor; IFR; liquid-metal reactor; LMR; metallic fuel; nuclear fuel cycle; plutonium; reactor design; reactor safety; recycling.

INTRODUCTION AND OVERVIEW

The first liquid-metal-cooled fast reactors (LMRs) used metallic fuel, but in the late 1960s—before the full potential of metallic fuels could be established—interest worldwide turned toward ceramic fuel for LMRs. At Argonne National Laboratory's (ANL) Experimental Breeder Reactor II (EBR-II), however, development of metallic fuels continued through the 1970s because the EBR-II test reactor continued to be fueled with the metallic uranium-fissium[1] alloy, U-5Fs. During that decade, the performance limitations of metallic fuel

* Work supported by the U.S. Department of Energy, Reactor Systems, Development, and Technology, under Contract No. W-31-109-ENG-38.

[1] Fissium is an alloy that approximates the equilibrium mixture of metallic fission product elements left by the pyrometallurgical recycling cycle designed for the EBR-II; it consists of 2.5 wt% molybdenum, 1.9 wt% ruthenium, 0.3 wt% rhodium, 0.2 wt% palladium, 0.1 wt% zirconium, and 0.01 wt% niobium.

for power reactor applications were satisfactorily resolved at EBR-II; in fact, additional attributes of metallic fuel were discovered. The results of the development work, both preceding and throughout the 1970s, have been summarized by Walters *et al.* (1984).

At the outset of the 1980s, it appeared that metallic fuel would remain second choice in the development of LMRs, despite the promise it showed. However, a series of events in the early 1980s caused a reassessment of reactor technology, including the LMR and its associated fuel cycle. Cancellation of the Clinch River Breeder Reactor (CRBR) in the U.S. signaled the need for this reassessment, and subsequent events reinforced that signal. From a purely economic viewpoint, the CRBR and the fuel cycle it represented had been seriously questioned. When the cost and inherent institutional implications of a large, centrally located recycling plant to service several LMRs became fully apparent, the need for such an enterprise evaporated. Furthermore, events at Three Mile Island (TMI) and Chernobyl demanded that an advanced reactor be demonstrably safer than any reactor of the current generation. Finally, increasing desire for environmental protection caused a reexamination of existing solutions to the disposal of radioactive waste.

In 1983, a concept called the Integral Fast Reactor (IFR) emerged at Argonne National Laboratory (ANL), offering a potentially safe and economical solution to the technical and institutional issues that have prevented nuclear power from fully contributing to the world's energy demands (Till and Chang, 1988; Chang, 1989). Central to the concept is recognition that the world's reserve of ^{238}U must be utilized as an energy source in the centuries to come. Thus, the fuel system must be able to utilize plutonium as its principal fuel and must have the potential to simultaneously create replacement plutonium by irradiating ^{238}U.

Metallic fuel appeared to be the most suitable candidate for the integral concept, and the U-Pu-Zr system, which had been under development in the late 1960s, was chosen over other metallic fuel systems because it promised superior performance. Excellent neutron economy and high burnup capability had been seen to be attributes of metallic fuel prior to 1983, and additional features of metallic fuel realized during the formulation of the IFR concept made metallic fuels all the more attractive.

In the first place, compared to oxide fuel, metallic fuel has a high thermal conductivity with very significant safety benefits (see Chapter 4). These benefits were demonstrated at EBR-II when test accidents were initiated at full power, with the loss of primary flow in one test and loss of heat sink in another, each without scram; in both cases, the reactor shut itself down without operator or mechanical intervention.

In the second place, metallic fuel lends itself to straightforward recycling by a novel technique that has several inherent advantages (see Chapter 7). The key step in the processing of metallic fuel is electrorefining. The cathode product contains uranium, plutonium, and the minor actinides, along with residual fission products. The bulk of the fission products are separated from the cathode product, permitting satisfactory nuclear performance of the recycled reactor fuel. The retained fission products keep the fuel highly radioactive, requiring that all recycling and refabrication steps be carried out remotely in a hot cell.

This recycling technology brings with it several benefits. First, undetected diversion of the fuel is virtually impossible since the material is highly radioactive; use of the material for nuclear weapons is not feasible because further PUREX-type reprocessing would still be required to separate plutonium from the uranium and remaining fission products (see Chapter 12). Second, the process involves batch operations, and thus is easily scaled to meet local requirements. Furthermore, comparative cost analysis has shown the process to be very competitive, relative to other recycling options.

Finally, and perhaps of greatest importance, this recycling method allows essentially all the actinides to remain in the fuel cycle, to be fabricated back into the recycled fuel and fissioned for useful energy (see Chapter 8). As a result, the high-level waste that emerges will decay to background in only hundreds of years, rather than tens of thousands.

Through the advantages mentioned above, metallic fuel offers solutions to a number of technical or institutional problems that, early on, had been thought to be inherent in LMRs. However, feasibility of the entire IFR concept, including safety, recycling, and fuel performance, required demonstration. An aggressive program was initiated in 1984 to prove the commercial feasibility of all aspects of the IFR concept, including a demonstration that U-Pu-Zr metallic fuel could meet all the requirements.

IFR FUEL SELECTION

Choice of Alloy

Obviously, there will be plutonium in a reactor whose fuel contains ^{238}U, a "fertile" material; however, the low melting temperatures of pure plutonium and pure uranium-plutonium alloys make it impractical to design a commercially attractive reactor that uses only those materials. Thus an additive was sought that would increase the melting temperature of the U-Pu alloys. Several elements that alloy well in this system were explored. Chromium, molybdenum, titanium, and zirconium all resulted in an adequate increase in melting temperature over a satisfactory range of plutonium content in the alloy. However, zirconium was unique in that it enhanced compatibility between the fuel and austenitic stainless-steel cladding materials by suppressing the interdiffusion of fuel and cladding components (Walter *et al.*, 1975). Without zirconium, the cladding elements nickel and iron readily diffuse into the fuel to form compositions that result in a lower solidus temperature (the temperature at which melting starts) adjacent to the cladding. Should the solidus temperature at the fuel/cladding interface be exceeded during an off-normal event, the cladding could fail due to penetration by the liquid front. The concentration of zirconium in the U–Pu-Zr alloys was limited to about 10 wt% for plutonium concentrations of up to 20 wt%, because too much zirconium would result in a liquidus temperature (the temperature at which melting is complete) that would exceed the softening point of the fused-quartz molds in the injection-casting fabrication equipment used for metallic fuel (Tracy *et al.*, 1989). By the end of the 1960s, a plutonium-based fuel alloy had been partially developed that had both adequate compatibility with the cladding and a high solidus temperature.

Raising the melting temperature solved only part of the difficulty—there remained the need to achieve high burnup and long residence time in the reactor. Eventually that was accomplished by a simple change in design, based on theoretical developments in the early 1960s (Blake, 1961; Barnes, 1964): the initial smeared density[2] was reduced (Hofman, 1980).

The metallic fuels first used in the experimental breeder reactors EBR-I and EBR-II, in the Fermi nuclear power station, and in the Dounreay Fast Reactor (DFR) had high smeared density (initially 85 to 100%), with little or no gap between fuel and cladding. Even at low burnup, the cladding deformed and failed when the fuel swelled from accumulation of fission products. Attempts at that time to extend the burnup were concentrated on alloying, on thermomechanical treatment of the fuel to suppress swelling, and on the use of strong cladding to resist deformation and the onset of swelling. That work was largely unsuccessful, peak burnups of about 3 at% being the best achievable.

In fuel without fabrication texture, the primary cause of swelling is the accumulation of fission-product gas in bubbles that grow as gas pressure increases with burnup and overcomes the gas-bubble surface tension, causing the fuel matrix to expand. It was known theoretically that when fuel swelling reaches about 30%,

---

[2] "Smeared density," a dimensionless percentage, is commonly used to quantify the effective density of the fuel within the cladding. As used here, it denotes a planar smeared density calculated by dividing the mass of fuel (including any nongaseous fission products) in a unit length of pin by the theoretical mass of a unit length of voidless fuel of the same composition, with diameter equal to the inside diameter of the cladding. Low smeared density can be achieved by using highly porous fuel or a large gap between fuel and cladding. Note that the smeared density increases as burnup proceeds because each heavy-metal atom that fissions becomes two atoms of a less dense material.

the bubbles must begin to interconnect, independent of size and number density. Therefore, it was postulated that if the gap between fuel and cladding were large enough to allow the fuel to swell about 30% before fuel/cladding contact, the bubbles would interconnect and release the accumulated fission gas, thus removing or reducing the primary cause of swelling; a large gas plenum above the fuel would capture the fission gas and keep the stress on the cladding reasonably low. By the time the metallic fuel development program was terminated in the late 1960s, it had been demonstrated that interconnection of pores and subsequent release of fission gas occurred consistently when the smeared density was less than 75% for a range of metallic fuel alloys.

Thus, by the close of the 1960s, solutions of performance problems associated with metallic fuels had been proven feasible—but had not been demonstrated with a large number of fuel pins irradiated to high burnups: only about 18 fuel pins had reached a burnup of as much as 4 at% in a fast reactor without failure before the metallic fuel development program was terminated (Walter *et al.*, 1975). ANL proposed that the core of EBR-II be converted to U-Pu-Zr fuel, clad with austenitic stainless steel, at a smeared density of 75%, with a large gas plenum at the top of the fuel pin. This would replace the uranium-fissium (U-5 wt% Fs) fuel designated as MK-IA beginning in 1970. The MK-IA fuel was clad with austenitic stainless steel with an 85% smeared density and had a very small gas plenum. Because of the low burnup achievable with the MK-IA fuel, the decision was made by the U.S. Atomic Energy Commission (AEC) that mixed-oxide fuel would be developed as the nation's fast reactor fuel. However, it was convenient to continue to use metal fuel for EBR-II, which would continue operations as a test reactor for mixed-oxide fuel and advanced cladding material. It was economically desirable to convert the core of EBR-II from the high smeared density MK-IA fuel to a low smeared density fuel that could go to higher burnup, but to keep the fuel composition U-5 wt% Fs instead of U-Pu-Zr (Walter *et al.*, 1973). As a result of that decision, a MK-II fuel design emerged in 1970 for use in EBR-II. The MK-II was U-5 wt% Fs at a smeared density of 75%, first clad with 304 of stainless steel and later with 316 stainless steel, with a plenum-to-fuel volume ratio of about 0.6. By 1974 it was clear that the new design was successful. Cladding breach did not occur until about 10 at% burnup, more than a factor of three better than the MK-IA fuel.

The most common breach mode for the MK-II fuel was a small intergranular crack in the cladding at the restrainer dimples—three small, sharp-bottomed indentations that were placed 120° apart about 2 cm above the fuel column (Seidel and Einziger, 1977). Their purpose was to prevent the metallic fuel pin from somehow ratcheting upward inside the cladding, then dropping back down at an inopportune time and creating a reactivity insertion. However, post irradiation examination of a large number of MK-II fuel pins showed only a slight upward motion in a small number of them; thus, future designs eliminated any type of restraining device. Later, fuel irradiated without the restrainer dimples achieved substantially greater burnup.

More than 30,000 MK-II fuel pins have been irradiated in EBR-II as standard driver fuel, with consistently excellent results (Seidel *et al.*, 1986 a,b). The administrative burnup limit for the fuel remained at 8 at%, even though consistently no cladding breach occurred below 10 at%. The burnup limit of 8 at% was chosen for two reasons. First, the "hex" (hexagonal) ducts on the fuel assemblies were initially made of Type 304 stainless steel. At a fuel burnup of 8 at% (about 8×10^{22} n/cm^2 total), the diameter of the hex ducts had increased from radiation-induced swelling until they could not be handled through the in-vessel EBR-II storage basket. Second, 8 at% was far enough below the ultimate burnup capability of 10.5 at% to assure that the probability of in-reactor breach was very low during steady-state operation, and to provide a wide margin for containing all anticipated effects of off-normal events. With these safeguards in place throughout the 1970s, EBR-II continued to demonstrate that metallic fuel is capable of high burnup.

As mentioned earlier, the IFR concept restored interest in metallic fuel. However, as of 1983 the commercial viability of U-Pu-Zr fuel remained undemonstrated, even though many of the feasibility questions associated with the performance of metallic fuel had already been answered. In fact, additional positive attributes of metallic fuel had been discovered, such as robust performance during off-normal transients. Nevertheless, from 1969 to 1984 no U-Pu-Zr fuel was irradiated and there was no facility available to fabricate the fuel.

With only 18 U-Pu-Zr fuel pins irradiated to about 4 at% burnup, the data base was weak, although these fuel pins did exhibit the performance that would have allowed them to reach high burnup. Moreover, in addition to the lack of demonstration that the U-Pu-Zr fuel would, in fact, reach high burnup, a number of other issues required further study for complete resolution.

In 1984, as a result of a broad reassessment of the constraints inhibiting nuclear power deployment, Argonne initiated work on the IFR (see Chapter 1). In conjunction with this, capability to fabricate ternary fuel was established, and a fuel program to demonstrate performance was initiated to gain the information that would be needed to eventually obtain a license for metallic fuel from the Nuclear Regulatory Commission (NRC). A number of assemblies were irradiated to establish the burnup potential of the U-Pu-Zr fuel, and how the fuel pins would perform with alternative cladding materials and with a range of design parameters such as smeared density, plenum-to-fuel volume ratio, operating temperature, and linear power. Finally, there was a series of tests to help develop the fuel fabrication specifications. In parallel with the irradiation experimentation, analytical modeling and out-of-core testing were undertaken to improve understanding of fuel performance.

For the initial set of three tests of U-Pu-Zr fuel, the irradiation began in EBR-II in early 1985, and a burnup of 18.4 at% was reached (Pahl *et al.*, 1990 a,b). The test contained fuel of three compositions: U-10Zr, U-8Pu-10Zr, and U-19Pu-10Zr (compositions given in weight percent). The fuel was clad with an austenitic stainless steel alloy, D9. Later in 1985, a test with fuel identical to the first three, but with cladding of the martensitic alloy HT9, began its irradiation in EBR-II. Fuel elements clad with HT9 reached 17.5 at% burnup without cladding breach.

A great deal of information, discussed in depth in later sections, was accumulated from the postirradiation examination of these initial assemblies. It was found that although the microstructure of the alloys was strongly dependent on their composition, the quantity of gas released to the plenum as a function of burnup was consistent for all fuel alloys irradiated, as was the burnup at which the pores became interconnected. Further, it was observed that the initial swelling of the fuel, up to the point of fuel/cladding contact, was anisotropic, with the radial component more than twice as large as the axial component (Hofman *et al.*, 1990). Still, the fuel slug had appreciable axial growth as a function of alloy composition and irradiation conditions. As expected from irradiation results in the 1960s, radial redistribution of the alloying elements was observed, particularly uranium and zirconium, although the radial concentration profile of plutonium was largely unchanged (Porter *et al.*, 1990). As the radial concentration of zirconium and uranium changed, a radial distribution of porosity developed, with distinct zones that were evident on a macro scale. Up to the burnups examined, the changes in the diameter of the austenitic cladding could be attributed primarily to radiation-induced swelling and creep, the source of stress being the plenum pressure in the fuel pin.

Up to a burnup of 18 at%, it appeared that any contribution to the strain in austenitic cladding from fuel/cladding mechanical interaction (FCMI) was insignificant (see below). Cladding-strain data are available for fuel pins with martensitic cladding, up to a burnup of 16 at%. At that burnup no swelling is expected; indeed the observed cladding strains were small, and could be attributed largely to creep due to plenum-pressure stress alone.

Uranium-Plutonium Metallurgy

Pure uranium metal is not used as fast reactor fuel, but fast reactors operating on a closed fuel cycle will, by their very nature, contain significant amounts of plutonium. Uranium, however, remains the major constituent of the alloy, and the properties of uranium's solid-state phases are reflected in the behavior of its alloys under irradiation. It is therefore instructive to lead off discussion of other metallic fast reactor fuel with a short review of earlier work on uranium and its alloys.

Uranium has three allotropic forms between room temperature and its melting point: A cubic, high-temperature γ phase, an intermediate-temperature tetragonal β phase, and a low-temperature orthorhombic α phase. Metal-fueled reactors operate in a temperature range where all three phases may be present.

The most important irradiation characteristic of α uranium is its dimensional instability, showing up as anisotropic growth and swelling due to the anisotropic properties of the orthorhombic crystal structure (Kulcinsky *et al.*, 1969). In a polycrystalline sample, the growth of individual grains results in shape changes, and thereby in mismatched strains between the individual grains. The stress due to these mismatched strains can be released by plastic deformation at the grain boundaries, commonly referred to as tearing or cavitation.

This type of swelling is characterized by large, irregular cavities, resulting in a very deformed, "swirled" microstructure, as shown in Fig. 1 (Bellamy, 1962; Leggett *et al.*, 1967). Because cavitational swelling is related to anisotropic growth in α uranium, it is influenced by the preferred grain orientation and the stress during irradiation. Cavitational swelling is not fission-gas driven, being basically a process that occurs at moderate temperature (~500°C). Because the tears are almost empty, material that has undergone cavitational swelling is relatively compressible. However, at higher burnup, fission gas will collect in the preformed cavities, pressurize them, and impart bubble-like properties to them. Unless the fission gas can escape, the buildup of internal pressure will make the fuel less compressible.

In contrast to swelling in the α phase, swelling in the higher temperature phases occurs by growth of fission-gas bubbles—except, of course, the swelling that takes place throughout all phases due to solid and liquid fission products (Greenwood, 1962; Claudson *et al.*, 1959). Fission gas is virtually insoluble in metallic uranium, and although a certain concentration of gas may be held in dynamic solution as a result of fissioning, fission gas will precipitate as bubbles, some of which then grow by acquiring more gas atoms. At some burnup level, when sufficient fission gas has been generated, the gas bubbles tend to maintain an equilibrium pressure by balancing internal pressure P_i against bubble surface tension γ and external pressure P_{ex} through growth (i.e. increase in bubble radius r) according to the equilibrium relation expressed in Eq. 1:

$$P_i = P_{ex} + \frac{2\gamma}{r}. \qquad (1)$$

The external pressure is determined by the plastic-flow characteristics of the fuel surrounding the bubble (Enderby, 1956) and by the pressure of the medium external to the fuel (Kulcinsky *et al.*, 1969; Lehmann *et al.*, 1968; Leggett *et al.*, 1966). This mechanism can lead to very high swelling rates at high temperatures, where fission-gas diffusivity and vacancy mobility are high and the fuel matrix strength, which in externally unrestrained fuel determines P_{ex}, is low, as is the case for the γ phase.

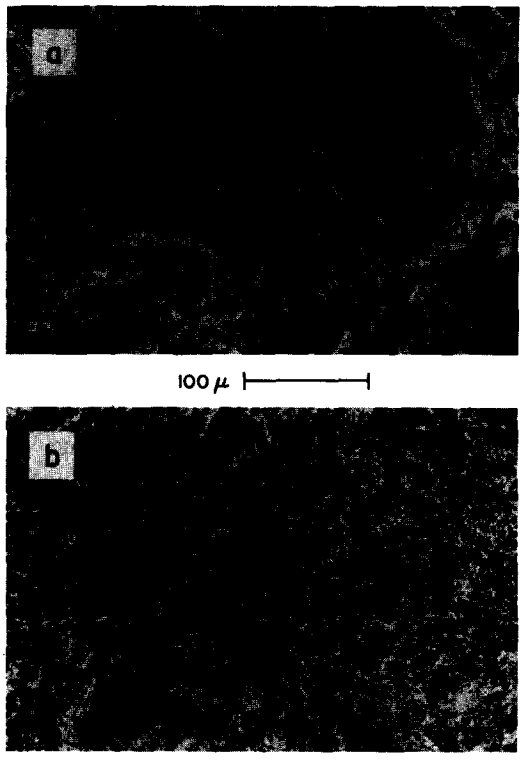

Fig. 1. Cavities Formed in Unalloyed Uranium and a Low-Silicon Alloy During Irradiation.
a. Unalloyed uranium, 1250 MWd/T.
b. U with 150 ppm Fe and 100 ppm Si, 2130 MWd/T.

Plutonium is soluble in concentrations up to 16% in α uranium, and the α-uranium phase retains its anisotropic characteristics. Plutonium is soluble up to 20% in β and completely in γ uranium. Alloys with up to 16% plutonium can, therefore, be expected to have swelling behavior similar to uranium. Irradiation experiments confirm this (Pugh, 1961). In the α phase, cavitation dominates, whereas rapid growth of fission-gas bubbles dominates in the γ phase. It appears that the addition of plutonium enhances the swelling rate in each of the phases, presumably because plutonium increases the diffusivity in the alloy and decreases the creep strength. At higher plutonium concentrations, the orthorhombic α phase of the alloy transforms to a tetragonal δ phase; as a result, the cavitational component diminishes as the anisotropic α phase disappears. Binary U-Pu alloys, however, are not suitable for high-temperature application because of their relatively low melting points, and because of the eutectics plutonium forms with commonly used iron- and nickel-based cladding materials. This may be improved by adding certain nonfissile elements to the binary alloy and by inserting diffusion barriers such as tungsten and vanadium between fuel and cladding. Considerable data on candidate alloying materials are available from the early work on ternary alloys that was carried out to solve the then-paramount swelling problem.

Irradiation Induced Swelling

Attempts to reduce swelling of plutonium-containing fuels for fast reactors by means of alloying have been generally unsuccessful. Researchers in the U.K. (Frost *et al.*, 1962) and France (Mustelier, 1962) concentrated on U-Pu-Mo, basing their choice on prior experience with U-Mo alloys. Large swelling, as much as 100%, occurred in these alloys at burnups of ~1 at% in the temperature range of interest, 500 to 700°C. The swelling was due to extensive fission-gas porosity similar to that found in high temperature γ-U irradiations. Work in the U.S. focused on U-Pu-Fs, U-Pu-Ti, and U-Pu-Zr, with similar results (Horak *et al.*, 1962; Beck *et al.*, 1968).

A search for a better cladding method was undertaken—a way to control excessive swelling caused by both cavitation and high-temperature fission-gas bubbles. Since the primary function of cladding is to provide a radiological barrier between fuel and coolant, it should also withstand the stress that comes with its secondary role as a restraint to fuel swelling. It is clear from Eq. 1 that if more free volume is provided inside the cladding to accommodate swollen fuel, the internal gas pressure P_i will be lower at a given burnup. At an appreciable average bubble size, γ/r will be relatively small, and the external pressure P_{ex} provided by cladding restraint will then be nearly equal to P_i. This model was worked out by Blake (1961), who showed that a burnup of ~5 at% (at that time a significant improvement) would be achievable with metallic fuel if approximately 30 to 40% free volume were provided for fuel swelling. Blake did not consider gas release in his model, but when Beck *et al.* (1968), following a suggestion by Barnes (1958, 1964), showed that most of the fission gas was released from the fuel at ~30%

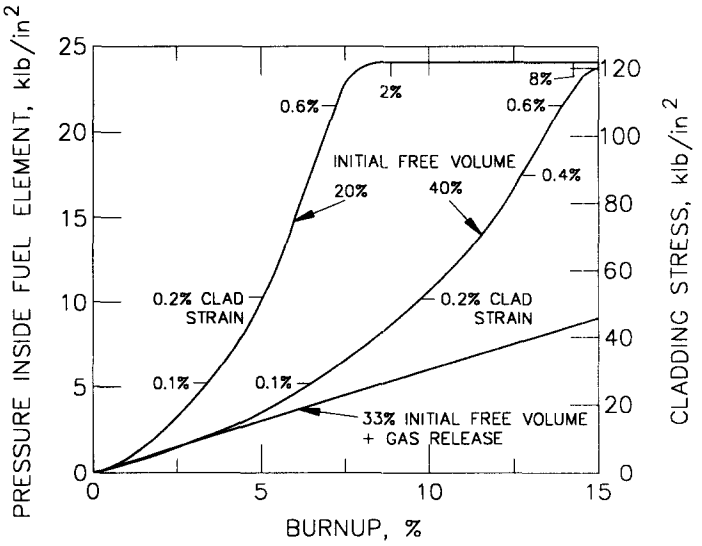

Fig. 2. Variation of Fuel Pressure Inside Cladding as a Function of Burnup (Blake, 1961). (Temperature 500° C; wall thickness/diameter ratio 0.09.)

swelling, it was clear that the pressure inside the fuel pin could be decreased by providing a plenum for this gas.

Given a fuel pin with a gas-plenum volume equal to the original fuel volume (plenum-to-fuel volume ratio of one), Blake's model yields the cladding pressure loading and strains, with and without release of gas to the plenum, shown in Fig. 2. Although the actual cladding stress and strain depend on the dimensions and type of cladding and on irradiation-enhanced creep and swelling of the cladding (which Blake did not consider), it is clear that the large reduction in cladding deformation due to gas release makes a truly high-burnup operation possible. A large amount of free volume in a tubular fuel pin is normally provided by a suitable gap between fuel and cladding. In order to improve the transfer of heat from fuel to cladding, this gap is filled with a liquid metal such as sodium. The plenum above the fuel should be large enough to accommodate this sodium when expelled from the gap by the swelling fuel, while leaving sufficient volume to accommodate released fission gas.

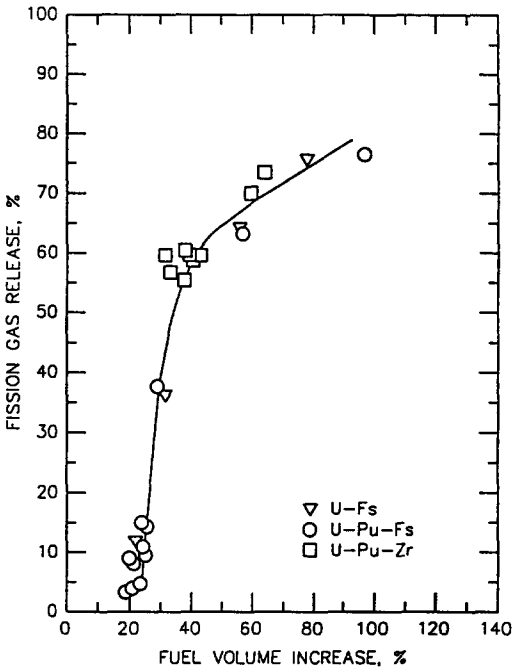

Fig. 3. Fission-Gas Release Versus Fuel-Volume Increase (Beck, 1968).

Although there is no longer a need to reduce swelling to achieve high burnup, these early experiments were important in characterizing the development of interconnected pores and attendant release of gas in various alloys. The correlation of gas release with swelling appears to be rather independent of fuel alloy, as shown in Fig. 3. In addition, the swelling measurements were useful in designing follow-on fuel pins, permitting more accurate prediction of increase in fuel length and of the burnup to be expected before fuel and cladding come in contact.

PERFORMANCE CHARACTERISTICS OF IFR FUEL

Swelling and Gas Release

As the only metallic fuel alloy currently under active study, U-Pu-Zr has the most extensive data, although substantially older data for U-Fs and limited information on other alloys are available. The general swelling behavior for these alloys is shown as the increase of fuel length versus burnup in Fig. 4. Swelling proceeds rather rapidly with burnup, a characteristic of metal fuel. Virtually all length increase takes place during the burnup interval before the swelling fuel contacts the cladding, which occurs at ~1% burnup. For a given type of fuel, the leveling off in axial swelling is thus determined by the fuel's initial smeared density. The initial smeared density is typically chosen to be approximately 75%, to allow enough swelling (approximately 30%) to release the fission gas from the fuel (see Fig. 3). This much planar swelling would, if it were isotropic, translate to a length increase of approximately 15%. However, the observed length increases are consistently smaller, indicating anisotropic swelling. The main reason for this appears to be the difference in swelling behavior between the hotter center of the fuel and the colder periphery, illustrated in Fig. 5 for U-10Zr (Hofman *et al.*, 1990).

In the center part of the fuel, where the γ phase predominates, large gas bubbles form, indicating higher plasticity of the fuel and therefore lower capability to withstand shear stresses. In the extreme, if the center

were to behave in a viscous manner the fission-gas pressure in the center would result in a biaxial loading of the peripheral shell, the radial stress component being twice the axial component. Stress-induced swelling in the peripheral fuel zone (predominantly α phase) would result in a larger diametral than axial strain; hence, anisotropic swelling (Kobayashi *et al.*, 1990). Anisotropy is especially pronounced and variable in U-Pu-Zr, as can be seen in Fig. 4. Note that the diameter of the fuel expanded some 15% to reach the cladding while the axial growth was only 2 to 8%, as shown in the figure.

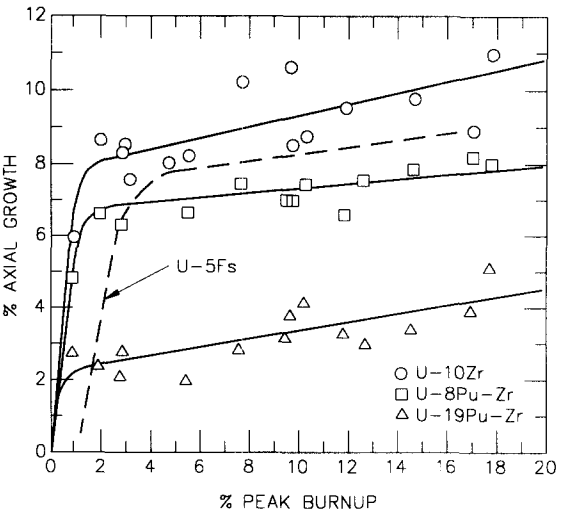

Fig. 4. Fuel Length Increases in Various Metallic Fuels as a Function of Burnup. (EBR-II irradiation. All the fuels had similar initial smeared density.)

The larger anisotropy (proportionately low axial swelling) in some of the higher-plutonium pins is because a radial distribution of alloy phases develops, a result of rather rapid redistribution of zirconium in the radial temperature gradient. This is consistent with the equilibrium phase diagram of U-Pu-Zr, which shows that various phase-field boundaries can be found radially across an operating fuel pin. The solubility of zirconium in these phases varies with temperature; thus, a driving force for diffusion can be created both by the gradient in chemical potential of the fuel constituents in these phases, and by the heat flow. A low-zirconium zone consisting primarily of plutonium in the δ phase is observed to form at the center of pins by zirconium migration to the lower temperature δ-phase zirconium at the periphery. In parts of fuel pins that operate at higher temperatures, the zirconium-depleted zone forms at midradius by migration of zirconium to both the high temperature γ-phase zirconium at the center and the δ-phase zirconium at the periphery.

The boundaries of the radial zones follow isotherms in the fuel, which determine the various phase boundaries of the alloy. In the usual situation of upward coolant flow and a cosine-shaped axial power profile in the fuel, the peak fuel temperature occurs between the center and top of the fuel column. An example of the resulting zone pattern in a moderate power U-19Pu-10Zr fuel pin is shown in Fig. 5. In higher power pins where the peak fuel temperature shifts to a higher axial position, the three-zone pattern, with a zirconium-depleted zone at an intermediate radial location, may extend to the very top of the fuel column.

Migration of the constituents of alloys in a temperature gradient, the so-called Soret effect, is rather difficult to measure experimentally in most alloy systems because of its extremely slow kinetics. However, such migration is commonly observed in power reactor fuel, owing to a combination of large temperature gradients and, possibly, fission-enhanced diffusivity. Examples are migration of fission products in mixed oxide fuel (Hehenkamp, 1977) and redistribution of hydrogen in U-Zr hydride fuel (Merten *et al.*, 1963). The chemical driving force for redistribution of a particular solute in a homogeneous solution held in a temperature gradient arises from the temperature dependence of the solute's chemical potential, and from transfer of energy by conduction electrons and photons. Such a system will tend to minimize its total free energy by adjusting its composition, thereby producing a chemical potential that is constant. The solute flux in a temperature gradient is characterized by a phenomenological parameter, called the "effective heat of transport" Q* of the the migrating solute, according to Fick's first law:

$$J_i = \frac{-D_i N_i}{RT}\left[\frac{RT\,\partial[\ell n(N_i)]}{\partial x} + \frac{Q^*}{T}\frac{dT}{dx}\right], \qquad (2)$$

where D_i and $\ell n(N_i)$ are the diffusivity and logarithmic concentration of the migrating solute.

The heat of transport can be positive or negative depending on the sign and magnitude of its components. For example, the value of Q* was measured to be -34 kcal per mole for pure uranium (D'Amico and Huntington, 1969) and +5 kcal per mole for zirconium (Campbell and Huntington, 1969). In their pure states, uranium moves down a temperature gradient and zirconium moves up. Whether this has any significance for a U-Zr alloy we would not hazard to speculate. Thus far, a valid model that takes into account all contributions to Q* has eluded researchers. In the absence of a model that is capable of predicting direction and magnitude of thermomigration in the present fuel alloys, we may use a phenomenological approach developed by Shewmon (1958) for two-phase alloys to explain our observations. With appropriate assumptions, Eq. (2) may be written as:

$$J_i = -\frac{DN_i}{RT^2}[\Delta\bar{H}_i + Q^*]\frac{dT}{dx}\,, \tag{3}$$

where $\Delta\bar{H}_i$ is the partial molar enthalpy of solution for component i. The migration direction is thus determined by the sign of the sum $[\Delta\bar{H}_i + Q_i^*]$.

The rate of zirconium redistribution in low-plutonium fuel (3 and 8%) is similar to the rate in U-10Zr, but it is much more rapid for plutonium concentrations of 19% and higher. Fig. 5 shows fuel with 19% Pu at only 3% burnup, to be contrasted with the binary fuel shown in Fig. 6 at 5% burnup; both of these pins were irradiated at the same power density (i.e., same temperature gradient and fission rate). Either higher zirconium diffusivity in the higher plutonium alloys or a larger thermodynamic force due to the presence of β-phase plutonium may account for this more rapid redistribution. The combined effect of the temperature gradient dT/dx and the fission-enhanced diffusivity D on the kinetics of the redistribution is evident from the observation that significant zirconium migration and zone formation in lower power density high-plutonium fuel pins is slower than that at high power density (Porter *et al.*, 1990). The available data cannot distinguish between the effects of temperature gradient and diffusivity.

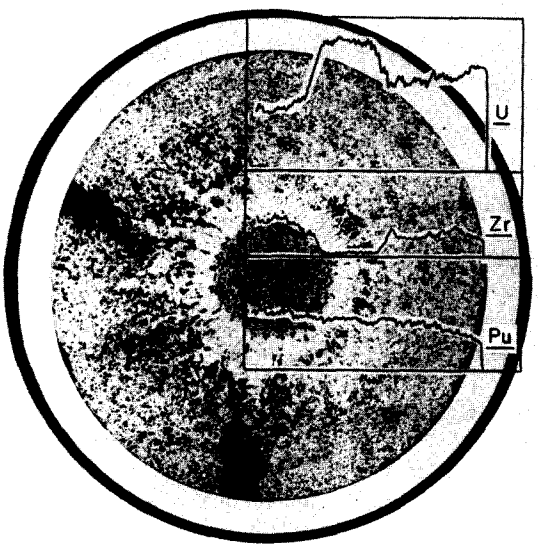

Fig. 5. Transverse Metallographic Section from the High-Temperature Region of a U-19Pu-10Zr Element at 3 at.% Burnup, with Superimposed Microprobe Scans, Showing Zone Formation, Cracking and Zr-U Redistribution.

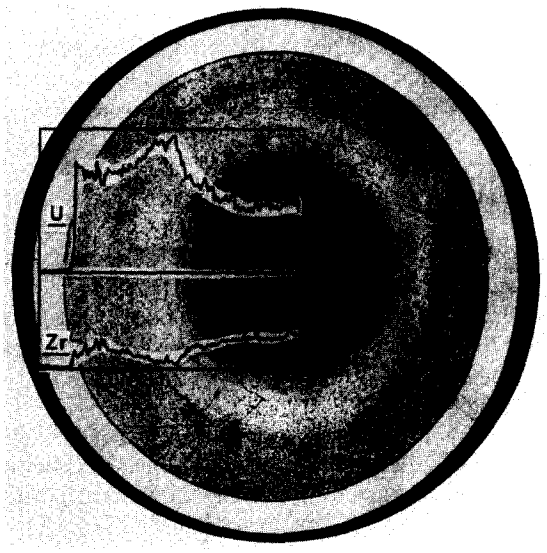

Fig. 6. Transverse Metallographic Section from the High-Temperature Region of a U-10Zr Element at 5 at.% Burnup, with Superimposed Microprobe Scans, Showing Zone Formation and Zr-U Redistribution.

If, as in high-plutonium high power density fuel pins, zone formation occurs rapidly (i.e., early on in the irradiation during the swelling stage prior to fuel/cladding contact), it enhances the rate of radial swelling markedly. This high rate of radial swelling increases the swelling anisotropy and creates stresses in the peripheral fuel large enough to result in crack formation, as shown in Fig. 5.

The development of porosity in metallic LMR fuel depends on the phases present in the fuel. In all alloys, the high-temperature cubic γ-phase uranium exhibits the characteristic large interconnected bubbles similar to those observed in pure γ uranium. At lower temperatures where the α-phase uranium predominates, the characteristic tearing type of porosity is evident. In U-Zr and U-Pu-Zr, the low temperature uranium α and zirconium δ phases form a laminar microstructure with rather smaller interlaminar spacing in U-Zr than in U-Pu-Zr, and the pore morphology follows this microstructure. Examples of both high and low temperature porosity in U-Zr and U-Pu-Zr fuel are shown in Figs. 7 and 8. When zirconium redistributes and phasal zones form, the resultant low-zirconium β and δ phases of plutonium have their own very fine pore morphology, an apparent characteristic of many intermetallic compounds (Hofman *et al.*, 1986).

A proper description or model of swelling and gas release should include the behavior of the various phases present, and requires, therefore, a rather precise thermal calculation to determine the phase fields in the fuel pin. A model for redistribution of alloy constituents and the formation of new phases, such as the δ phase

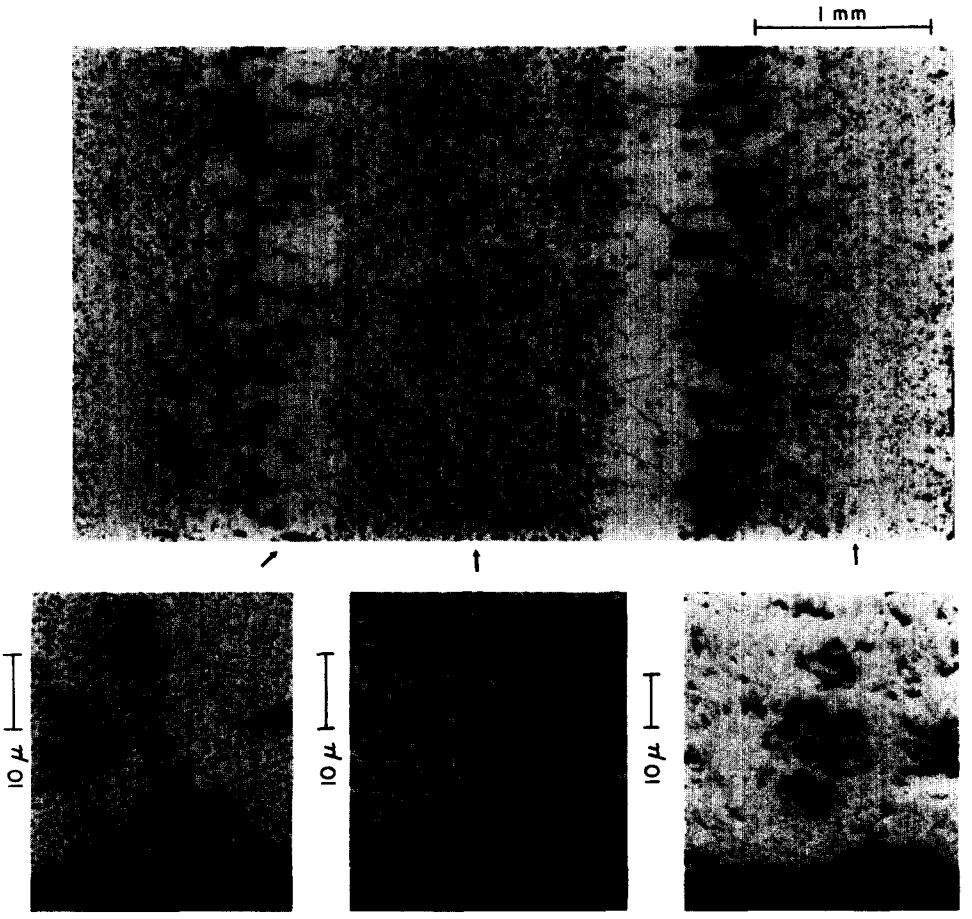

Fig. 7. Redistribution and Zone Formation in U-19Pu-10Zr Fuel at 3 at.% Burnup; Transverse Optical Metallographic Section. (Central: High temperature.)

in U-Pu-Zr, is also essential. These needs call attention to the difficulty of determining the thermal conductivity of the fuel during irradiation, a classic problem in the modeling of any fuel pin. For example, the thermal conductivity of mixed-oxide fast reactor fuel changes during irradiation because of pore formation, fuel restructuring, stoichiometry changes, and buildup of fission products. Also, changes in the heat conductance of the fuel/cladding gap have important impact on the efficiency with which heat is removed from the fuel. A satisfactory description of these changes in mixed-oxide fuel has taken a great deal of effort.

A detailed evaluation of thermal conductivity of metallic fuel would be fraught with similar difficulties; fortunately most of the performance parameters of metal fuel pins are adequately determined from the average conductivity of the fuel. With the porosity in the various microstructural zones in the fuel well characterized by postirradiation examination, the drop in thermal conductivity due to porosity can be calculated with existing models (DiNovi, 1972). The gap conductance in sodium-bonded metallic fuel pins is very high, and plays no significant role in the overall thermal calculation. If, however, the sodium bond were locally displaced by fission gas, the gap conductance would decrease at those locations. This sort of displacement appears plausible, as evidenced by the local irregularities in the fuel microstructure commonly observed in postirradiation metallography of high-plutonium pins that exhibit the aforementioned rapid redistribution and cracking; such irregularities are not observed in fuel not afflicted by cracking. For example, U-10Zr fuel develops an axial, cone-shaped zone structure that follows isotherms within the fuel.

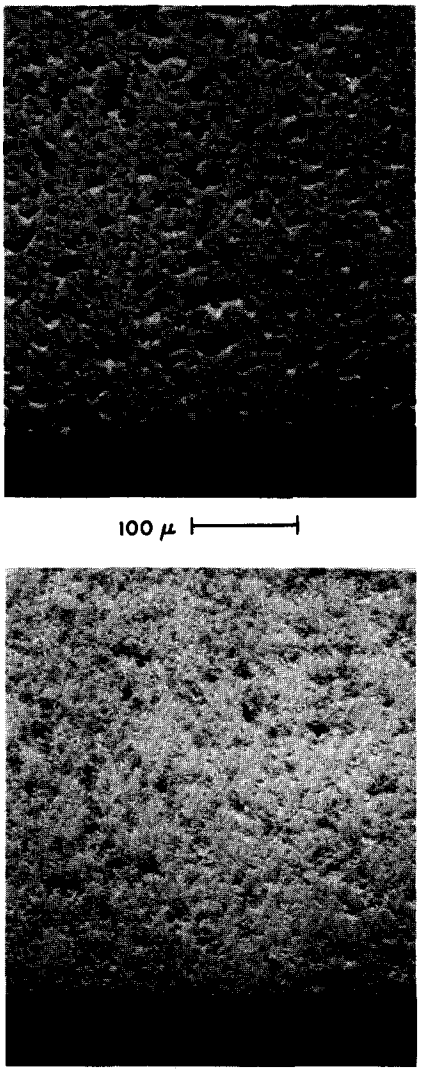

Fig. 8. Different Pore Morphologies in Irradiated U-10Zr, Predominantly γ Phase (high temperature) (upper) and Predominantly α Phase (low temperature) (lower). (Scanning electron microscopy.)

Effect of the Sodium Bond

The bond sodium also plays an important role in the thermal behavior of fuel during irradiation by assuring that the thermal conductivity remains reasonably high throughout the burnup cycle. An important concern is that the large amount of swelling and porosity developed during the first few atom-percent of burnup may lead to large reductions in the thermal conductivity of the fuel. During this free-swelling stage, bond sodium is displaced from the gap to the gas plenum above the fuel. Later, as swelling proceeds, the pores in most of the fuel interconnect, and gas is vented to the plenum. Eventually, near the point of maximum swelling, the pore interconnections become large enough to allow the bond sodium to infiltrate the body of the fuel. This ingress of high-conductivity bond sodium into the fuel porosity effectively restores much of the thermal conductivity that the fuel lost in the initial free-swelling stage.

Evidence for this behavior of bond sodium comes from a variety of sources. Sodium infiltration is routinely observed in postirradiation examination. The sodium level above the fuel in pins where the fuel has swollen out to the cladding is always substantially lower than the total amount of preloaded sodium would indicate,

and chemical analysis of irradiated fuel finds this "missing" sodium distributed throughout the fuel. Direct measurements of the radial temperature drop in specially constructed U-5Fs fuel pins equipped with thermocouples at the fuel center and the outer surface of the cladding in the ANL CP-5 reactor (Beck and Fousek, 1969) and in EBR-II (Betten, 1985), both show sudden drops in central fuel temperature, indicative of sodium logging at burnups associated with interconnecting porosity and fission gas release.

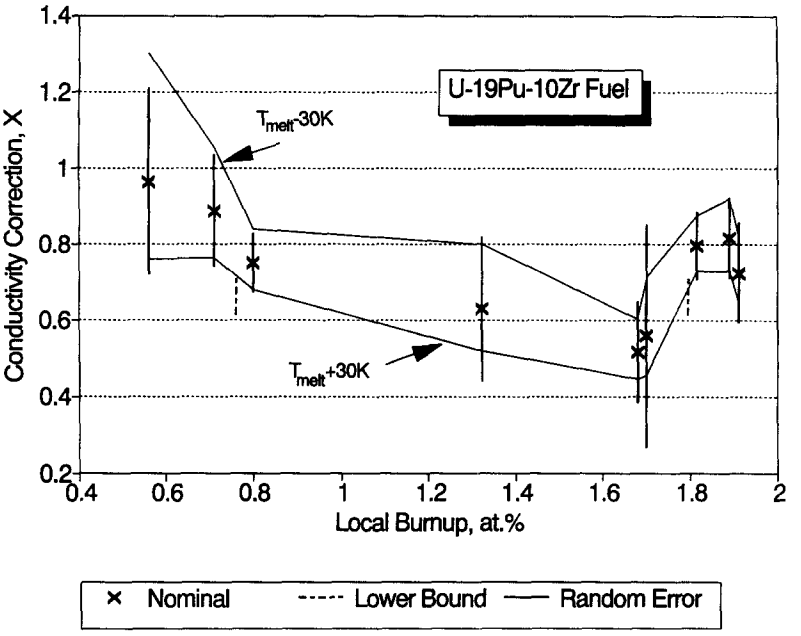

Fig. 9. Measured Thermal Conductivity Correction as a Fraction of Nominal Thermal Conductivity of Unirradiated Fuel versus Local Burnup for IFR Ternary Fuel. (Bauer and Holland, 1995)

More recently, Bauer and Holland (1992, 1995) determined the thermal conductivity of IFR U-Pu-Zr and U-Zr fuel by examining fuel pins that remained intact after transient-overpower testing in TREAT, basing their deductions on metallographic examination to determine the extent of fuel melting, combined with careful thermal-hydraulic analysis of well-instrumented experiments (described later). These results, illustrated by Fig. 9, were used to quantitatively correlate the fuel's thermal conductivity with burnup, and they directly support the notion that thermal conductivity of the fuel drops steadily in the early stages of burnup, followed by sudden increases caused by sodium ingress. The figure indicates the effect of an assumed systematic uncertainty in fuel melting temperature as well as estimated 1 σ random errors.

Further changes at high burnup depend primarily on the type of cladding used, as illustrated in Fig. 10. High-swelling cladding such as austenitic stainless steel allows further radial swelling of the fuel, which provides additional room for buildup of solid fission products. Low-swelling cladding, such as martensitic HT9 steel, restricts the swelling of the fuel, so that the porosity gradually decreases due to the buildup of these fission products.

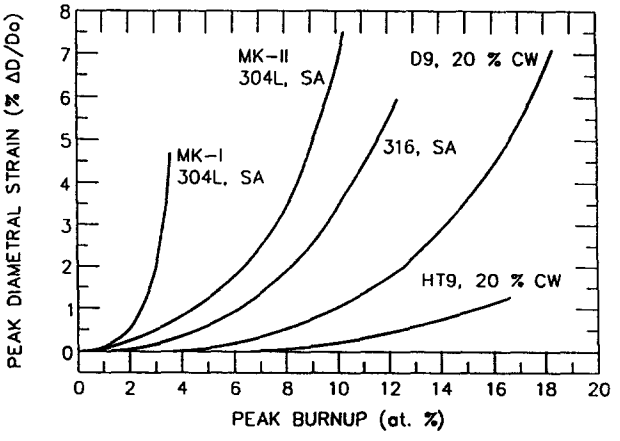

Fig. 10. Progressive Improvement in the Deformation (Swelling and Creep) of the Cladding of Metallic Fuel Elements (EBR-II Irradiations). (SA: solution annealed; CW: cold-worked.)

Another aberration in the thermal conductivity of the fuel can occur if transverse cracks form at various locations along its length. An example of this is shown in Fig. 11.

From the variation in radial location of the microstructure zones, it appears that less sodium was logged at the crack, probably because of locally trapped fission gas.

FUEL/CLADDING INTERACTION

Interaction between fuel and cladding that may lead to cladding failure can be both mechanical and chemical. Fuel/cladding mechanical interaction (FCMI) arises from applied stress when the cladding is designed to restrain fuel swelling, and may result in plastic deformation of the cladding.

Fuel/Cladding Mechanical Interaction

The major source of stress in metallic fuel is the buildup of fission gas in bubbles or existing tears. Internal fission-gas pressure builds rapidly with burnup, and metallic fuel is rather plastic during fissioning. Because early pin designs did not allow the fuel sufficient room for free swelling, this gas-bubble pressure was transmitted directly to the cladding. As a result, all early designs suffered from cladding deformation and rupture at modest burnups. However, as discussed earlier, an as-built smeared density of about 75% allows free fuel swelling of approximately 33%, at which point porosity becomes largely interconnected and open to the outside of the fuel, releasing a large fraction of the fission gas to a suitably large plenum at the top of the pin. The gas pressure in the open pores is then determined by the volume and temperature of the plenum above the fuel.

A series of irradiation experiments was performed in the CP-5 reactor to test this idea (Beck *et al.*, 1968). Pins containing U-Pu-Fs, U-Pu-Ti, and U-Pu-Zr were included in this series, with a variety of cladding materials and a range of smeared densities and plenum volumes. If the effects of fuel/cladding chemical interactions are excluded, a consistent picture emerges from these tests. High-burnup operation (in excess

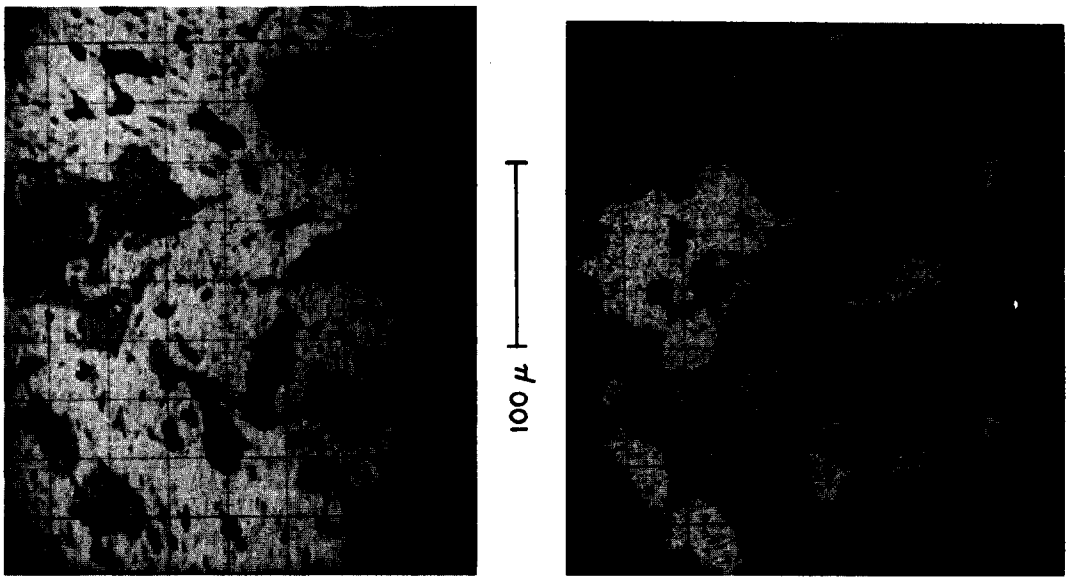

Backscatter Cerium X-ray

Fig. 11. SEM Scans of U-19Pu-10Zr Fuel with 17 at.% Burnup.

of 10 at%) without cladding failure is achievable with smeared densities of 75% or lower and plenum-to-fuel volume ratio of 0.6 or higher. A subsequent test based on these parameters with U-Pu-Zr pins was successfully run in EBR-II (Murphy *et al.*, 1969). On the basis of these confirming results, the EBR-II driver fuel pin was changed from the MK-IA (smeared density 86%; plenum-to-fuel volume ratio 0.15) to the MK-II type (smeared density 75% and plenum-to-fuel volume ratio 0.15). The cladding deformation as a function of smeared density, using U-5Fs fuel and Type 304 stainless-steel cladding, is shown in Fig. 12.

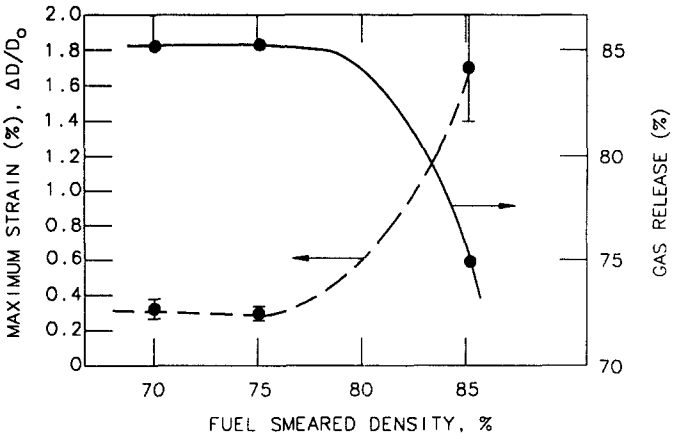

Fig. 12. Peak Cladding Diameter Increase and Gas Release Fraction for HT-9-clad U-19Pu-10Zr Fuel of Various As-built Smeared Densities, at 12.5 at% Burnup. (Tsai, 1991)

The cladding strain of the low smeared density, small-plenum MK-IA design is primarily creep strain due to FCMI, while that of the MK-II pins is mainly radiation-induced swelling of the cladding. The creep strain in the MK-II pins can be accounted for by plenum pressure alone, which confirms that FCMI is virtually nonexistent in suitably designed metallic fuel pins, and that cladding stress is determined by the fission-gas pressure in the plenum and interconnected porosity.

Since open (interconnected) fission-gas porosity appears to be a key feature in reducing FCMI, the question arises as to what the effect of accumulation of low-density solid fission products on this porosity might be at high burnup. The following discussion contains an approximate calculation of the net volume change due to accumulation of nongaseous fission products.

The volume changes and total yield of the major nonvolatile, nonsoluble fission products are shown in Table 1. A rigorous analysis of the change in molar volume of the fuel due to transmutation of uranium and plutonium into solid fission products requires evaluation of the fission products' chemical state in the various metallurgical phases—a difficult task, considering the complexity of the alloys. However, an approximation for the major fission products can be made if one partitions these products and makes the following assumptions: (1) Zirconium, niobium, and molybdenum are all in solution in the fuel phases, and thus contribute some to the swelling by reducing the density of the fuel; (2) alkali elements are partly dissolved in the bond sodium; (3) the noble metals precipitate as compounds; (4) the rare earths precipitate as a separate compound or alloy; and (5) the majority of the alkaline earths precipitate separately. Post-irradiation examinations of high-burnup fuel appear largely to support both this partitioning and these assumptions. Another reason for partitioning the fission products is their different migration behavior in the fuel; such grouping allows evaluation of the effect this migration has on the properties of the various radial phasal zones. The accommodation of the nonsoluble fission products predictably results in expansion as a function of burnup. However, the lattice is depleted in uranium and plutonium as fissioning proceeds, resulting in a volume decrease that partially offsets the expansion due to fission products.

Further, it was assumed that all the fission-product zirconium, niobium, and molybdenum are soluble in the matrix, and that they compensate for some of the volume decrease due to the loss of the uranium and plutonium that has fissioned. Thus, nongaseous fission products contribute to the volume change in three ways:

- Volume decrease due to the fissioning of uranium and plutonium;

Table 1. Volume Changes Due to Nonsoluble Major Fission Products

Element group	Fission yield per 100 fissions	State	Average molar volume cm^3 $mole^{-1}$	Percent volume change per % BU*
Alkali (Cs, Rb)	22.2	Liquid, 70% in Na bond	70	0.108
Alkaline Earth (Sr, Ba)	14.7	Solid, Liquid, in Precipitation and 20% in Na	20	0.146
Rare Earths + Pd (Ce, Nd, etc.)	51.4	Solid, Precipitation	20	0.792
(Tc, Ru, Rh, Ag)	23.3	Solid, Precipitation	9	0.162
Total nonsoluble fission products:				1.18

* For a molar volume of 12.9 cm^3 $mole^{-1}$ of U-19Pu-10Zr.

- volume increase due to the increase of zirconium, niobium, and molybdenum, which are soluble in the fuel matrix;
- volume increase due to nonsoluble fission products.

The result of the first two contributions is estimated as follows: at 10 at% burnup of the uranium and plutonium, the average composition of the U-19Pu-10Zr (wt%) fuel matrix has changed from 77(U-Pu)-23Zr at% to 71(U-Pu)29(Zr-Nb-Mo) at%, with an associated volume change of -0.2% per percent burnup.

As shown in Fig. 11 for a U-19Pu-10Zr fuel sample with 17 at% burnup, the rare earths (represented by cerium in Fig. 11), which are insoluble, are found to collect in two separate phases, primarily in large pores toward the periphery of the fuel and in the gaps between fuel and cladding. Evidently these elements migrate down the temperature gradient. One of these two phases contains most of the palladium, but the other noble metals are concentrated in blocky precipitates throughout the fuel.

Molybdenum, zirconium, and niobium are not found as separate phases, and are thus probably in solution in the various fuel phases. Chemical analysis of bond sodium indicates that a major fraction of the alkali and some of the alkaline-earth elements can simply be added to the volume of the bond sodium. The changes in fuel volume due to these fission products are also given in Table 1. The increase in total volume due to the nonsoluble fission products amounts to approximately 1.2% of the fuel volume per percent burnup.

In addition, at any time during the irradiation there is a fraction of the xenon and krypton that has not found its way to the general porosity and thus resides in the fuel matrix. This gas is in solution and in very small agglomerations that act as a solid, liquid, or high-pressure gas. Moreover, the concentration of this resident fraction of the gas is probably very different in the various fuel phases, and has not been well characterized. Post-irradiation examination, however, including wet-chemical analysis of high-burnup fuel, indicates that 10% of the gas volume for an entire pin is a reasonable estimate of the average resident fraction. Such a fraction in solution and in liquid or nonideal dense gas increases the volume of the fuel by ~0.2% per percent burnup. This brings the total volume increase (not counting voids) to approximately (-0.2 + 1.2 + 0.2) = 1.2% per percent burnup.

As a result of this volume increase, assuming no cladding deformation occurs, an as-built smeared density of 75% of theoretical would change to 81% at 10 at% burnup, and 90% at 20 at% burnup. It appears that

in this high-burnup range, the initially open porosity will become increasingly closed off, and fission-gas pressure in the fuel will build more rapidly since less of the generated gas will vent to the plenum. In effect (remembering that the fuel has been in contact with cladding since ~1% burnup), this would represent the onset of possibly significant fuel/cladding mechanical interaction (FCMI). In irradiation of fuel that has a smeared density of 75%, FCMI has not been observed at burnups of up to 18%. This is readily explained for austenitic stainless steel cladding such as Type 316 and D9. As shown in Fig. 10, the deformation of the cladding steel at high burnup is so large that it accommodates any increase in the volume of the solid fuel. The deformation in Type 316 and D9 cladding is caused mainly by swelling, and any irradiation creep strain can be accounted for by plenum pressure alone; hence, no evidence of FCMI.

Because of the desire to keep cladding deformation low at high burnup (high fluence), a nonswelling martensitic stainless steel, HT9, is the current cladding material of choice for LMR fuel pins. As shown also in Fig. 10, the deformation at 16 at% burnup is only approximately 1%, and the smeared density of the fuel at this point should have changed from 75% to approximately 85%. Apparently little FCMI has occurred at this burnup, even with the nonswelling material, since the cladding creep strain can be accounted for by plenum pressure only, within the accuracy of the calculations. In order to determine the effective smeared density at which significant FCMI does occur, HT9-clad fuel pins with an initial smeared density of 85% were irradiated along with the usual 75% (Tsai, 1991). The resulting cladding strains are compared in Fig. 12. It is clear that the rate of growth of cladding strain increased for the initially 85% smeared-density pins, somewhere prior to 12% burnup, when solid fission products increased the smeared density from 85% to approximately 95%. It appears from these data that FCMI became substantial in this interval, although even for initial values of 85%, open porosity apparently develops to some extent, and substantial, albeit less, gas release occurs, as is shown in Fig. 12. Only when solid fission products increase the smeared density to well above 85% does FCMI become clearly evident. We may conclude that even with nonswelling cladding, significant FCMI can be avoided to high burnup if the as-built smeared density is kept to 75%. In this discussion it has been assumed that the porosity is uniformly affected by the accumulation of fission products. Clearly, based on the observed porosity patterns and the location of fission products in the fuel, this may be too simplistic for a precise evaluation of FCMI, but it appears adequate for analysis of both steady-state and transient performance.

Fuel/Cladding Chemical Interactions

Fuel/cladding chemical interaction (FCCI) in an all-metal fuel pin is in essence a complex, multicomponent diffusion problem. Characterization of fuel/cladding interdiffusion is exceedingly difficult, because of the number of alloy components involved. With stainless steel cladding, even in the simplest fuel alloys such as U-Fs and U-Zr, at least five major constituents participate in the diffusion process. In addition, minor alloy components such as carbon, nitrogen and oxygen, as well as fission products—particularly at higher burnup—appear to play an important role. The potential problem of interdiffusion of fuel and cladding components is essentially twofold: Weakening of cladding and formation of relatively low-melting-point compositions in the fuel. In an attempt to assess the severity of these two deleterious effects in preparation for irradiation testing of specific fuel pins, one customarily performs diffusion-couple experiments in the laboratory, involving specific interfacing samples exposed to heat or other accelerating influences.

During the 1960s, ANL tested a large number of fuel/cladding combinations with this diffusion-couple method. It was concluded that the 300 series of austenitic stainless-steel cladding has an acceptably low susceptibility to cladding attack with U-Fs fuel. However, the addition of plutonium increases the rate of attack, and, more important, decreases the temperature at which melting is observed in the diffusion zone.

These results, and earlier data reported by Kittel (1949) on diffusion experiments with uranium, led the researchers to conclude that nickel played an important role in fuel/cladding interdiffusion. These findings and conclusions are relevant to the newly developed low-swelling cladding materials. As shown in Table

2 (Zegler and Walter, 1967), a marked improvement in both diffusion rates and minimum melting temperature was obtained through the addition of at least 10 wt% zirconium in the fuel alloy, whereas titanium, which was also considered as a fuel alloy addition, proved to be ineffective. This discovery was an important factor in the selection of 10 wt% zirconium alloys for the present IFR fuels.

Table 2. Melting Temperatures from Diffusion-couple Data after 300-700 Hours at Temperature

	Melting Temperature (°C)			
	304	316	HT9	D9
U-8Pu-10Zr	>760	790	740	<750
U-19Pu-10Zr	>780	790	>780	>730
U-26Pu-10Zr	---	<775	650	650
U-15Pu-11Zr (1967)	>800	>800	>800	>800

In order to specifically assess the propensity to form molten phases, diffusion experiments were performed with the current IFR fuel/cladding combinations. Series-300 stainless steels were included, as well as fuel samples from an archive fuel pin that was fabricated in 1967 for comparison with the previous experiments. The results of these experiments are summarized in Table 2. They are reasonably consistent with the 1960s data: there is considerable scatter in both sets of data in regard to various fuel/cladding types, but the results fall in the same general range.

This type of testing has shown many indications of the influence of the formation of a surface layer of zirconium containing 20 to 30 at% of interstitial elements (oxygen, nitrogen, carbon), as was found in the 1960s studies (when oxygen was thought to play a dominant role). The interstitial element found in greatest abundance in the interface zirconium layers found in the recent work (Hofman *et al.*, 1986) was nitrogen. Moreover, it seemed that thicker layers were formed in couples where the nitrogen content of the cladding alloy was greatest. It was therefore speculated that the enhanced compatibility of the 316 couples was due to the 600 ppm nitrogen contents, versus 40 to 50 ppm in the HT9 and D9 alloys.

Studies have shown that small amounts of nitrogen in a heat-treatment atmosphere can induce the formation of zirconium-rich layers on the surface of samples. These layers were then shown to enhance compatibility in subsequent diffusion-couple tests, and they appear to be effective interdiffusion barriers. Variability in how the layers form as influenced by test technique, sample preparation, etc., may also explain some of the scatter in the diffusion-couple data.

Metallographic examination of the various diffusion couples leads to the following general observations (Hofman *et al.*, 1986): A zirconium layer containing approximately 20 at% nitrogen is first formed at the interface of all fuel/cladding combinations as shown in Fig. 13. This layer is thicker and apparently forms more readily in the case of Type 316 stainless steel, which has a rather high concentration of dissolved nitrogen. Subsequently, iron and nickel (in austenitic steels) diffuse into the zirconium layer and form two distinct phases that contain some uranium and plutonium as well, indicating that these elements can also diffuse through the zirconium compounds. Finally, further diffusion of uranium and plutonium leads to the formation of phases of mixed components of fuel and cladding equivalent to U_6Fe and UFe_2 on the cladding side of the zirconium compound layer.

The interdiffusion zones for Type 316 and D9 stainless steel differ in morphology and types of phases, and the rate of formation is much lower for the former, apparently due to the difference in the initially formed Zr-N layer. In the case of essentially nickel-free ferritic steel, HT9, the phases containing U-Fe_2 form a single zone. There exists a eutectic combination of these phases, the temperature of which depends on the concentration of plutonium and zirconium, as well as uranium and iron. However, judging from the data in Table 2 for D9 and HT9, this temperature appears to lie in the vicinity of the U-Fe eutectic—approximately 720°C. Presumably the Type 316 stainless steel would have yielded a similar melting temperature had the test run longer so that more uranium diffusion through the zirconium layer could occur. As it was,

melting in the case of Type 316 or 304L occurred near 800°C and appeared to have started in the fuel side of the diffusion couple. At this temperature, the diffusion of iron and nickel into the fuel, rather than uranium into the steel, led to eutectic formation. The eutectic temperature in the Fe-U-Pu-Zr system drops significantly with increasing plutonium concentration, which may explain the lower melting temperatures for the 26 wt% plutonium fuel. In this case also, the melting started on the fuel side of the diffusion couple.

The results obtained with diffusion couples indicate what might occur in a reactor during fuel/cladding chemical interaction. However, post-irradiation examinations and annealing experiments with irradiated fuel and cladding show significantly different behavior of FCCI in an actual fuel pin. The emphasis in the preceding discussion of the diffusion-couple test is on the formation of liquid phases, but, except during possible transient events, fuel pins operate by design below these melting points. The FCCI during normal operation is thus characterized by solid-state interdiffusion. As was suggested earlier, nickel appears to play an important role in FCCI. Preferential diffusion of nickel into the fuel leaves a ferritic layer in austenitic-steel cladding, regardless of the type of fuel. The nickel, as well as some iron, diffuses into the fuel to a depth several times as large as the nickel-depleted layer in the cladding. The ferritic layer, on the other hand, contains little or no fuel.

The effect of rare-earth fission products on nickel diffusion was considered because these elements are found in the nickel-depleted zone of austenitic-steel-clad U-Pu-Zr fuel pins up to a concentration of a few percent at 5 at% burnup (see Table 3), and as much as 20% in the high-burnup D9-clad pins (also reflected in the hardness of the nickel-depleted zone). Lanthanide (rare earth) fission products migrate readily to the cladding in plutonium-containing fuel, as shown in Fig. 11, but not as easily in U-Zr, which might explain the large difference in the thickness of the layer between those fuels and D9 cladding.

With austenitic and martensitic steel, FCCI has both similarities and differences. Because HT9 contains very little nickel, depletion of this element, which seems to control FCCI in austenitic D9, does not apply to HT9. However, the ferritic layer in D9 formed by nickel depletion is essentially similar to a ferritic layer in HT9 that results from decarburization of the original martensite. The differences in FCCI between austenitic and martensitic steel may be more significant than the aforementioned similarity. First, the rate of ferrite formation due to decarburization of HT9 is lower than that due to nickel depletion in D9 at comparable temperatures. Moreover, the diffusion of rare earths into the ferritic layers is quite different for the two steels. Unlike the uniform diffusion in D9, rare earths in HT9 diffuse only partially along a uniform front, but rather more along grain boundaries.

Although our understanding of FCCI is not complete at this juncture, it appears that the data allow us to make the following general observations: Prior to accumulation of significant amounts of lanthanide fission products at the fuel/cladding interface, FCCI depends on the particular fuel/cladding combinations; e.g., the degree of nickel depletion in austenitic cladding and decarburization of martensitic cladding has a solid-state diffusion-type of dependence on time and temperature. Lanthanides ultimately control FCCI, but their presence at the internal cladding surface depends not only on burnup but very strongly on their radial migration in the fuel. Although radial migration of lanthanides increases with fuel temperature for all fuel alloys, it is more rapid in U-Pu-Zr than in U-Zr.

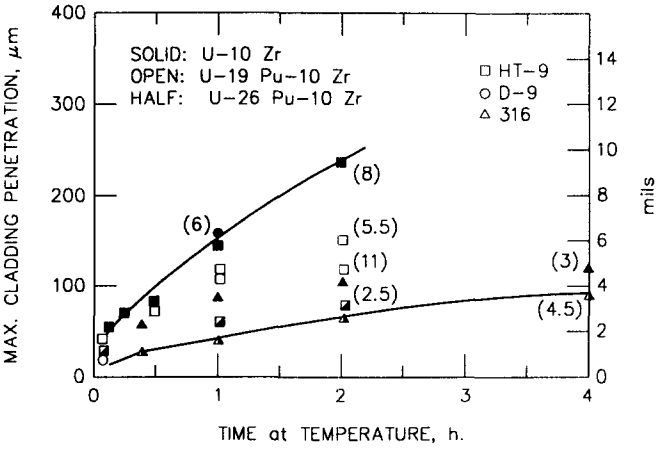

Fig. 13. Envelope of Depth of Penetration by Fuel/Cladding Melt into the Cladding as a Function of Time at 800°C during Post-irradiation Heating Test (Tsai, 1991). (In parentheses: percent burnup of test samples.)

Table 3. Comparison of Nickel-Depleted (Ferritic) Zones in Various Fuel/Cladding Combinations

Fuel	Cladding	Ni-depleted zone, μ	Burnup, at%	T(BOL) °C	Ce-Nd at%	Hardness DPH
U-15Pu-9Zr	304L	140	5	650	few	280
	316	30	5	650	few	280
U-9Pu-10Zr	D9	100	17	580	~20	1050
	316	70	13	580	NM	1000
U-10Zr	D9	20	17	580	NM	NM
U-10Zr	HT9*	100	5	650	3	200
U-19Pu-10Zr	HT-9	45	12	600	NM	350

Notes: NM Not measured
* Decarburized zone for HT-9

The in-situ formation of Zr-N layers in diffusion couples and the reduced nickel depletion found in Type 316 stainless steel indicate the feasibility of improving the FCCI. However, the FCCI problem with austenitic cladding might be largely academic, since swelling alone renders these steels unacceptable for use at high burnup. High-burnup operation requires a low-swelling cladding material such as HT9, so acceptable FCCI is more important in this steel.

Although melting due to FCCI is not expected at normal operating conditions, the ex-reactor diffusion tests indicate that liquid-phase formation needs to be taken into account if cladding temperatures reach the 700 to 800°C range during transient conditions. In the transients that were considered, the temperatures in this range are reached in events that last only minutes, while lower temperature events, such as loss of coolant combined with a disabled heat-rejection system, may last many hours. To better characterize the formation of liquid phases in cladding and fuel at elevated temperatures, sections of various irradiated fuel pins have been heated in an in-cell apparatus over a range of temperature and time (Tsai, 1990). This work has shown no evidence of liquid-phase formation below ~725°C for test durations of up to 7h, in general agreement with the diffusion experiments discussed before, and has yielded a large body of kinetic data at higher temperature (Tsai, 1991). Figure 13 shows an envelope of the results of measurements on several fuel/cladding combinations, as a function of time at 800°C. The broadness of the data range is due to the number of fuel/cladding combinations tested—0-26% plutonium and Type 316, D9 and HT9 steels, as well as various burnup levels and irradiation conditions. Further testing is in progress.

In general, the penetration depths appear to be parabolic functions of time raised to a power of less than one. The rate of attack is similar for HT9 and D9, but generally lower for Type 316 with all fuel compositions. It is interesting to note that for the range of parameters covered thus far in these post-irradiation heating tests, fuel with 0% plutonium has shown the highest rate of attack and 26% plutonium the lowest, opposite to the trend observed in diffusion couples. Metallographic examination of these irradiated samples reveals that the FCCI is similar to that observed in unirradiated diffusion-couple tests, with the exception of a pronounced effect of rare-earth fission products in high-burnup fuel samples. This experimental program has not yet led to development of a satisfactory fundamental model for the observations. Meanwhile, correlations of cladding penetration with temperature and time derived from these preliminary test results are used empirically in evaluating transient behavior of metallic fuel pins.

TRANSIENT TESTING IN TREAT

Safety Tests

Safety tests in support of the liquid-metal-cooled fast reactor have been conducted in Argonne's Transient Reactor Test (TREAT) facility (Lambert *et al.*, 1990; Sackett *et al.*, 1990) for more than 20 years, using loops of flowing sodium. Beginning in 1985, safety studies of metal-fueled LMRs were undertaken within the IFR program, and six loop experiments in TREAT have been performed so far on irradiated metal fuel of modern design. These have been designated as the M-series tests M2 through M7 (Bauer *et al.*, 1990). All six were designed to provide data pertaining to transient-overpower-without-scram (TOP-WS) conditions in an IFR type of reactor. The specific objective was to study the behavior of fuel and cladding near the cladding-failure threshold, for a wide range of burnup and for several fuel/cladding combinations. Achieving this objective required, for some fuel pins, stopping the power transient at the brink of failure, and, for others, stopping the transient immediately after failure.

TREAT is a uranium-and-graphite-fueled reactor with a nearly thermal neutron spectrum. Its forced-air cooling system provides limited heat rejection capability. However, its two pairs of very fast-operating, computer-driven control rods provide capability for a wide range of power transients applicable for investigating most reactor safety issues. Most experiments involving transients require use of the fast-neutron hodoscope facility (DeVolpi *et al.*, 1982), and therefore the core needs to have a slot running from the experiment vehicle at the center of the core to the hodoscope collimator at the edge. The TREAT hodoscope is a system designed to collimate and detect fast neutrons born in fissions in the test fuel. It is used primarily to monitor motion of the test fuel inside experiment vehicles during transient experiments. The M-series tests were performed in a highly instrumented recirculating sodium loop at the center of the core.

All test fuel in this series was subjected to similar overpower conditions: full coolant flow and an exponential power rise on an 8-s period. While anticipated overpower transients in an IFR are likely to be much slower, the 8-s period was chosen as the slowest transient possible that would commence from near-nominal conditions and carry through to cladding failure within the energy deposition limitations of the TREAT reactor. Baseline thermal conditions in the test fuel were typical of nominal conditions in a fast reactor. These include a peak linear power rating of 40 kW/m, an inlet temperature of 630°K, and a 150°K coolant temperature rise. As stated earlier, the power rise was rapidly terminated upon detection of cladding breach, or, by using previously measured failure thresholds, just prior to failure. Fifteen pins have been tested; five were overheated to cladding breach, which in every case occurred near the top of the fuel. Power levels achieved in each case were in the neighborhood of four times nominal.

A comprehensive summary of the peak overpower conditions and the fuel performance observed in the test series is given in Table 4. Pin failures, when they occurred, are noted. Peak overpower levels reported for each test pin are given as multiples of the nominal fast reactor conditions given above.

Analysis of the tests indicates that melting of approximately one-half of the total fuel inventory encompassing over 90% of the cross section of the fuel slug near the top of the fuel was typical of what had been predicted for test pins in this series. Posttest examination of pins that remained intact confirmed these estimates. As described earlier, these measurements and analyses were also used to deduce the thermal conductivity of the fuel and to confirm the presence of bond sodium in restructured fuel (Bauer and Holland, 1992).

Cladding-failure threshold in metal fuel has been modeled on the basis of both overpressure and penetration by a low-temperature iron-uranium eutectic. In contrast to ceramic fuels, the lower mechanical strength of metal fuel leads to pressure in the pin plenum as the primary pressure loading of the cladding. Cladding strains, however, reflect not only the pin-plenum pressure but also thinning by eutectic formation. Cladding deformation and strain-to-failure are computed on the basis of stress/temperature history and correlations derived from transient tube-burst tests.

Table 4. Peak Overpower Conditions and Fuel Performance Results.

Fuel/Cladding	Axial Peak Burnup (at%)	Peak Overpower Threshold[a]	Calc. Failure Threshold (normalized [a,b])	Peak Pressure (MPa)[c]	Max Axial Expansion (%)
	fresh	3.8	4.3	0.6	4(d)
U-5Fs/	0.3	4.1	4.7	0.6-0.8	16
316SS	0.3	4.1	4.8	0.6-0.8	18
	2.4	4.1(e)	4.4	1-6	7
	4.4	4.2(e)	4.5	7-9	(f)
	4.4	4.0	4.4	7-9	4
	4.4	3.8	4.3	7-9	4
	7.9	4.1(e)	3.6-4.0	17-20	3
	7.9	3.4	3.6-4.0	17-23	4
U-19Pu-10Zr/	0.8	4.3	5.1	1	1
D9 Steel	1.9	4.3	5.0	3	3
	1.9	4.4	4.6	3	5
	5.3	4.4(e)	4.5	10	4
	9.8	4.0	4.4	19	2
U-10Zr/ HT9 Steel	2.9	4.8	4.4	6	3

Notes: (a) Multiple of normal operating power.
(b) Relative to nominal reactor conditions as stated in the text.
(c) Indicated uncertainty due to uncertainty in gas release fraction.
(d) Expansion may have been caused by localized sodium bond boiling.
(e) Cladding failure.
(f) Ambiguous data.

These concepts may be easily applied to the ongoing overpower test series. The high thermal conductivity of metal fuel assures that the peak cladding temperatures and, therefore, the likely failure sites will always be near the top of the fuel. Temperatures key to the failure-threshold analysis (pin plenum, peak cladding midwall, and cladding inner surface) are close to or easily derived from the measured whole-pin coolant-temperature rise. The rise rate is sufficiently rapid that, except at the highest possible burnups, failure would not be expected until the temperature of the fuel/cladding interface exceeds a threshold value of 1350°K, the temperature at which eutectic penetration into the cladding becomes very rapid (associated with the melting of a protective, solid, iron-uranium compound). Depending on the particular test or reactor conditions, this temperature is reached at overpower levels around four times nominal. Detailed calculations have been performed, and the predicted times (power levels) of cladding failure are reported in Table 4. While these calculations are not precise, observed overpowers at cladding failure were in reasonable agreement (±5%) with expectations, with the notable exception of the single U-Zr pin.

The survival of the U-Zr pin, which was tested to about 4.8 times nominal power, was quite unexpected—not only because calculated cladding failures have tended to lag behind observed failures, but also because computed temperatures far exceeded the expected threshold (1350°K) for rapid melt penetration. To obtain

the expected conditions for melt penetration, it is necessary that a molten phase rich in uranium be in contact with the cladding. It is possible that the high solidus temperature (around 1500°K) of binary fuel prevents or delays the onset of rapid penetration.

Table 4 also reports measurements of peak prefailure elongation made by the fast-neutron hodoscope for each test pin. Measured values, varying from a high of nearly 20% down to 2 to 3%, were in every case significantly beyond the approximate 1% attributable to pure thermal expansion. In most cases, the peak expansion persisted during cooldown and was evident in posttest remains. Measured expansion of irradiated U-Fs fuel showed strong dependence on burnup and was especially large at low burnup. By contrast, expansion of the IFR fuel was typically less and did not show large burnup dependence. In irradiated fuel, the underlying mechanism is believed to be expansion of fission gas that is initially confined within solid fuel, but freed to expand as fuel melts. (Expansion of the one "fresh" pin tested may have been caused by boiling of bond sodium that had mixed in with molten fuel.) Quantitatively, axial expansion is estimated by a model in which the fission gas in molten fuel simply expands until its pressure equals that of the pin plenum.

When cladding failed, post-failure events were characterized by rapid fuel dispersal, rapid coolant voiding, and partial flow blockage. Different types of fuel behaved similarly. In all cases, cladding failure was accompanied by a sudden, temporary reversal of coolant flow at the inlet. Pressure spikes were minor (less than 2 MPa) and were correlated with the plenum pressure in the failed pin, but lower by about one order of magnitude. In each case, about half of the fuel inventory was ejected through a small breach at the top of the fuel. The amount of disruption observed seems correlated with the amount of pin depressurization following failure. Under these circumstances, disruption could be driven either by expansion of trapped fission gas or by sudden boiling of the liquid bond sodium within the fuel.

To summarize, the M-series tests have permitted generation and validation of simple models of cladding failure and prefailure expansion. Failure threshold with the 8-s period overpower conditions is about four times nominal power over a wide range of burnups and fuel types. (However, additional modeling issues and questions arise when test fuel is overheated for longer times at lower temperatures.) Prefailure axial expansion of metal fuel is significantly greater than thermal expansion, with strong dependence on fuel type, especially at low burnup. Expansion of fission gas trapped in melting fuel seems to be the mechanism at work. For IFR fuel, expansion in the range of 2 to 4% was typical of all burnups tested. Finally, on a qualitative basis, post-failure motion was benignly dispersive in all metal fuel types tested.

Operation of Fuel Pins with Breached Cladding

Unlike oxide fuel, metallic fuel is chemically compatible with sodium reactor coolant, which is why sodium is used for a thermal bond between fuel and cladding; sodium coolant is not expected to react with metallic fuel if, for some reason, a cladding breach occurs. The behavior of failed metallic fuel pins during continued operation is thus governed by the properties of the fuel, its fission products, and the cladding, and is not affected by fuel-sodium reaction products.

Several so-called run-beyond-cladding-breach (RBCB) tests have been performed in EBR-II with U-Fs, U-Zr, and U-Pu-Zr fuel clad with Type 316, D9, and HT9 stainless steels (Batté and Hofman, 1990). The purpose of these tests was to confirm the expected benign behavior of metallic fuel pins during operation following cladding breach, and to characterize the release of fission gas, delayed-neutron emitters, and possibly fuel, from breached pins. Some pertinent parameters and results of these tests are summarized in Table 5.

To simulate cladding failures prior to the design end-of-life of a pin, an area on the cladding of a pre-irradiated pin is machined down to approximately 30 to 40 μm. Shortly after reinsertion in the reactor, cladding failure occurs in this thinned area. This is annunciated by both fission-gas and delayed-neutron (DN) signals on the reactor monitoring system. A typical pattern of these signals is shown in Fig. 14. It

Table 5. Summary of Run Beyond Cladding Breach (RBCB)

Experiment ID Number	XY-21A	XY-24	XY-27	X-482	X482A	X482B
Composition, wt%	U-5Fs	U-19Pu-10Zr	U-19Pu-10Zr	U-19Pu-10Zr	U-10Zr	U-19Pu-10Zr
Cladding material	316SS	316SS	316SS	D9	D9	HT9
Final burnup, at%	~9.3	~7.5	~6.0	14.4	13.5	13.5
Pin diameter, mm	4.4	4.4	4.4	5.8	5.8	5.8
No. of days breached	54	233	131	168	100	150
DN signal, cps (note a)	~30-40	(note b)	(note b)	~600	~700	(note c)
Weight loss, g (note d)	2.0	2.7	2.5	4.0	3.6	3.9
Peak cladding temp(°C).	550	550	550	600	600	600

Notes: (a)Counts above background.
(b) Unavailable due to instrument malfunction.
(c) None detected, breached at startup.
(d) Expulsion of bond sodium fission gas and cesium accounts for the weight loss; fuel loss was negligible.

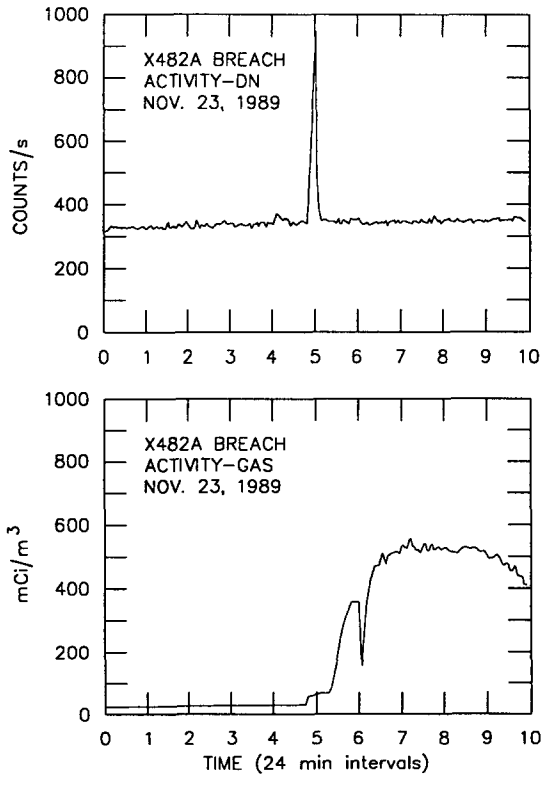

Fig. 14. Delayed-Neutron and Fission-Gas Signals Observed upon Breach of the Cladding of a High-Burnup Metallic Fuel Pin Irradiated in EBR-II.

consists of a short DN signal that coincides with the expulsion of bond sodium through the breach. After the bond sodium is gone, transport of delayed-neutron precursors to the breach site is slowed down enough that they decay before reaching the reactor coolant. A large portion of ^{133}Cs is expelled with the bond sodium, as reflected in a corresponding increase of this fission product in the reactor coolant.

Most of the long-halflife fission gas that collected in the pin during its earlier irradiation is also released in a short period following cladding breach, resulting in virtually complete depressurization of the pin. The long-term release is monitored by measuring fission gas isotopes as they are produced during the RBCB operation.

Because the pin is depressurized, and because FCMI is insignificant (since the fuel itself does not stress the cladding and there is no fuel-sodium reaction), there is little or no cladding stress during RBCB operations, particularly with high-swelling austenitic cladding. As a result, the cladding breach remains small, as shown in the top photo in Fig. 15, even after approximately 100 to 200 days of operation of the pins in the breached mode. A similar RBCB exposure within HT9-clad pins exhibited more crack extension and widening (bottom photo in Fig. 15). This may indicate a certain amount of FCMI resulting from trapped fission gas in closed-off porosity. This trapped gas also causes the fuel to swell somewhat at the breach site where the external restraining effect of the cladding has vanished. However, it is important

to note that no fuel was extruded through the cladding breach even after the 150 days of breached-pin operation.

Because of the expulsion of the bond sodium from breached pins, the sodium logged in the open fuel porosity also disappears (expelled by the expansion of trapped gas), and the thermal conductivity of the fuel slug, which had increased upon sodium logging, returns to a value commensurate with low-pressure gas-filled porosity. The main effect of the resulting increase in fuel temperature appears to be enhanced transport of rare-earth fission products to the periphery of the fuel slug, and an increase in FCCI. The depth of rare-earth penetration into the cladding at the top of the fuel after 150 to 200 days of RBCB operation is approximately twice that in unbreached pins at comparable burnup and cladding temperature. This is further indication that the behavior of rare-earth fission products plays an important role in FCCI.

SUMMARY

The ternary alloy U-Pu-Zr with a martensitic cladding such as HT9 appears to meet the essential requirements for IFR fuel. Its steady-state performance is outstanding and well understood. The fuel itself appears capable of essentially unlimited burnup, with lifetime ultimately set by a combination of pressure exerted on the cladding by fission gases accumulating in the plenum of the fuel pin and a fuel volume that increases by 1 to 2% per percent burnup from buildup of solid fission products. Performance in off-normal transients is benign, since major excursions lead promptly to fuel expansion driven by dissolved gases, without fuel-pin failure. At excessive temperatures there can be a chemical interaction of fuel and cladding, consisting of interdiffusion of some of their components. This, along with internal pressure from the fission gases in the plenum, is the ultimate mechanism for failure of a fuel pin. If a pin with breached cladding is subjected to continued operation, no further degradation occurs.

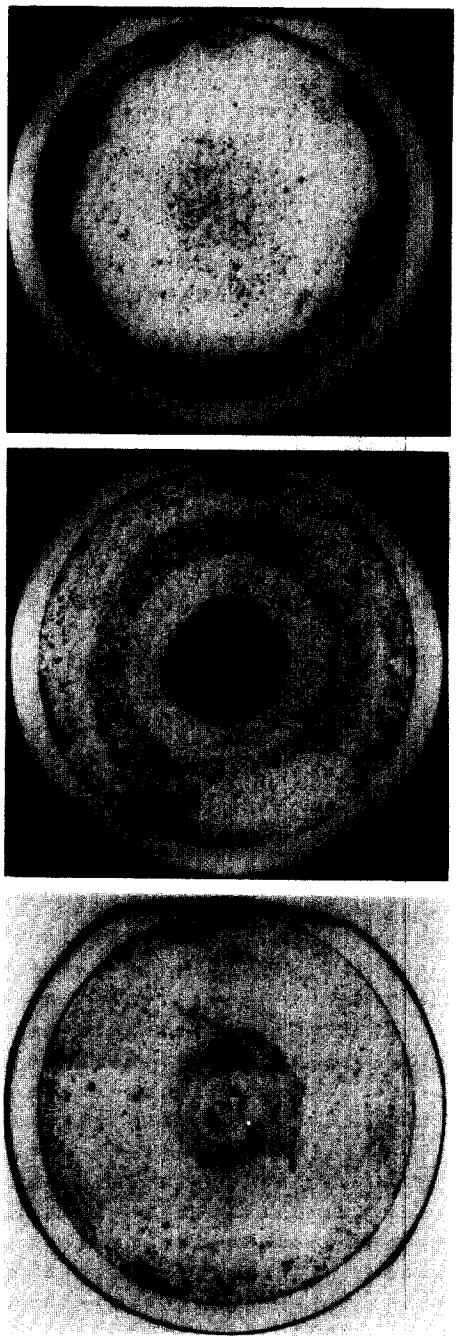

Fig. 15. Metallographic Cross Sections Through Cladding Breaches of Several Metallic Fuel Elements After Extensive RBCB Operation. (Flat section on cladding was machined to induce failure).

REFERENCES

Barnes, R.S. (1958). Swelling and Inert Gas Diffusion in Irradiated Uranium. *Proceedings of the 2nd United Nations International Conference on Peaceful Uses of Atomic Energy, Communique 5, No. 500*, Geneva, Switzerland, 1–13 September.

Barnes, R.S. (1964). A Theory of Swelling and Gas Release for Reactor Materials. *Journal of Nuclear Materials* **11**, 135.

Batté, G. and G.L. Hofman (1990). Run-Beyond-Cladding Breach (RBCB) Test Results for the Integral Fast Reactor (IFR) Metallic Fuels Program. *International Fast Reactor Safety Meeting IV*, p.207, Snowbird, Utah, 12–16 August.

Bauer, T.H. and J.W. Holland (1992). Integral Fast Reactor Metallic Fuel Program in Pile Measurement of the Thermal Conductivity of Irradiated Metallic Fuel. *Transactions of the American Nuclear Society* **65**, 278.

Bauer, T.H., A.E.,Wright, W.R. Robinson, J.W. Holland and E.A. Rhodes (1990). Behavior of Modern Metallic Fuel in TREAT Transient Power Tests. *Nuclear Technology 92*, 325.

Bauer, T.H. and J.W. Holland (1995). In-Pile Measurement of the Thermal Conductivity of Irradiated Metallic Fuel. *Nuclear Technology* **110**, 407.

Beck, W.N. R.J. Fousek and J.H. Kittel (1968). *The Irradiation Behavior of High-Burnup Uranium-Plutonium Alloy Prototype Fuel Elements*, Argonne National Laboratory Report ANL-7388.

Beck, W.N. and R.J. Fousek (1969). Fission Gas Release and Thermal Conductivity Measurements on U-5 Wt % Fs Irradiated in CP-5. *Transactions of the American Nuclear Society* **12**, 78.

Bellamy, R.G. (1962). The Swelling of Alpha-Uranium under Neutron Irradiation with 0.7% Burn-up. *Institute of Metallurgy Symposium on Uranium and Graphite*, London, England.

Betten, P.R. (1985). In-Core Measurements of Uranium - 5 wt.% Fissium Alloy Thermal Conductivity. *Transactions of the American Nuclear Society* **50**, 239.

Blake, L.R. (1961). Achieving High Burn-up in Fast Reactors. *Reactor Science and Technology* **14**, 31.

Campbell, D.R. and H.B Huntington (1969). Thermomigration and Electromigration in Zirconium. *Physical Review* **179**, 601.

Chang, Y.I. (1989). The Integral Fast Reactor. *Nuclear Technology* **88**, 129.

Claudson, T.T., G.T. Geering, J.W. Goffard and J.E. Minor (1959). *Operational Performance of Bonded and Unbonded Uranium Fuel Rods, Nuclear Metallurgy*, American Institute of Metallurgical Engineering, Chicago, Illinois.

D'Amico, J.F. and H.B. Huntington (1969). Electromigration and Thermomigration in Gamma Irradiation. *Journal of Physics and Chemistry of Solids* **30**, 1607.

DiNovi, R.A. (1972). *Effect of Burnup, Swelling and Irradiation Temperature on Thermal Diffusivity and Conductivity of Uranium-Fissium Alloy*, Argonne National Laboratory Report ANL-7889.

DeVolpi, A., C.L. Fink, G.E. Marsh, E.A Rhodes. and G.S. Stanford (1982). Fast-Neutron Hodoscope at TREAT: Methods for Quantitative Determination of Fuel Dispersal, *Nuclear Technology* **56**, 141.

Enderby, J.A. (1956). *Plastic Flow and Swelling of Gas Bubbles in Uranium*, U.K. Atomic Energy Authority Report ICR-R/R.198.

Frost, B.R.T., P.G. Mardon and L.E. Russell (1962). Research on the Fabrication, Properties, and Irradiation Behavior of Plutonium Fuels for the U.K. Reactor Programme. *Proceedings of the American Nuclear Society Meeting on Plutonium as a Power Reactor Fuel*, p.4.1, Richland, Washington, 13–14 September.

Greenwood, G.W. (1962). The Effects of Neutron Irradiation on λ-Uranium and Some Fissile Alloys of Cubic Crystal Structure. *Journal of Nuclear Materials* **6**-1, 26.

Hehenkamp, Th. (1977). *Electro- and Thermotransport in Metals and Alloys, AIME Symposium*, p.68, Niagara Falls, NY, 22 September.

Hofman, G.L. (1980). Irradiation Behavior of Experimental Mark-II EBR-II Driver Fuel. *Nuclear Technology* **47**, 7.

Hofman, G.L., A.C. Hins, D.L. Porter, L. Leibowitz and E.L. Wood (1986). Chemical Interaction of Metallic Fuel with Austenitic and Ferritic Stainless Steel Cladding. *Proceedings of the International Conference on Reliable Fuels for Liquid Metal Reactors*, p.12, Tucson, Arizona, 7 September.

Hofman, G.L., Pahl, R.G., Lahm, C.E. and Porter, D.L. (1990). Swelling Behavior of U-Pu-Zr Fuel. *Metallurgical Transactions A.* **21A**, 517.

Horak, J.A., J.H. Kittel and R.J. Dunworth (1962). *The Effects of Irradiation on Uranium-Plutonium-Fissium Fuel Alloys*, Argonne National Laboratory Report ANL-6429.

Kittel, J.H. (1949). *Layer Formation by Interdiffusion Between Some Reactor Construction Metals*, Argonne National Laboratory Report ANL-4937.

Kobayashi, T., M. Kinoshita and S. Hattori (1990). Development of the SESAMI Metallic Fuel Performance Code. *Nuclear Technology* **89**, 183.

Kulcinski, G.L., R.D. Leggett, C.R. Hann and B. Mastel (1969). Fission Gas Induced Swelling in Uranium at High Temperatures and Pressures. *Journal of Nuclear Materials* **30**, 3.

Lambert, J.D.B., W.K. Lehto, J.I. Sackett, D.J. Hill, H.P. Planchon and R.W. Lindsay (1990). EBR-II Test Programs. *International Fast Reactor Safety Meeting III*, p.181, Snowbird, Utah, 12–16 August.

Leggett, R.D., C.R. Hann, B. Mastel and K.R. Mereka (1966). *Swelling of Irradiated Fissionable Materials*, Battelle Northwest Report BNWL-207.

Leggett, R.D., T.K., Bierlein and B. Mastel (1967). Basic Swelling Studies, Radiation Effects. *American Institute of Metallurgical Engineering Symposium*, p.303, Asheville, North Carolina, September.

Lehmann, J.P. Paoli, N. Azam (1968). Etude du Gonflenent d'Alliages d'Uranium Sous Irradiation. *Journal of Nuclear Materials* **27**, 285.

Makin, M.J., W.H. Chatwin, J.H. Evans, B. Hudson and E.D. Hyam (1962). The Study of Irradiation Damage in Uranium by Electron Microscopy. *Institute of Metallurgy Symposium on Uranium and Graphite*, Paper No. 7, London, England.

Merten, U., J.C. Bokros, D.B. Couggisberg and A.P. Hatcher (1963). Thermal Migration of Hydrogen in Zirconium-Uranium-Hydrogen Alloys. *Journal of Nuclear Materials* **10**-3, 201.

Mikailoff, H. (1964). *Quelques Aspects du Gonflement en Pile des Materieux Fissiles*, CEA Rapport EEA 1601.

Murphy, W.F., W.M. Beck, S.L. Brown, B.T. Kopowski and L.A. Neimark (1969). *Post Irradiation Examination of U-Pu-Zr Fuel Elements Irradiated in EBR-II to 4.5 at % Burnup*, Argonne National Laboratory Report ANL-7602.

Mustelier, J.P. (1962). Quelques Resultes d'Irradiation Sur les Combustibles Evisages par Rapsodie. *Symposium on the Effects of Irradiation on Solids and Materials for Reactors*, p.163, Venice, Italy, 7 May.

O'Boyle D.R. and A.E. Dwight (1970). The Uranium-Plutonium-Zirconium Ternary Alloy System. *Plutonium 1970 and Other Actinides Nuclear Metallurgy, 17*, American Institute of Metallurgical Engineering.

Pahl, R.G., D.L. Porter, C.E. Lahm and Hofman, G.L. (1990a). Experimental Studies of U-Pu-Zr Fast Reactor Fuel Pins in EBR-II. *Metallurgical Transactions A. 21A*, 1863.

Pahl, R.G., R.S. Wisner, M.C. Billone and G.L. Hofman (1990b). Steady-State Irradiation Testing of U-Pu-Zr Fuel to >18 at% Burnup. *Proceedings of the International Conference Fast Reactor Safety IV*, 129, Snowbird, Utah, 12–16 August.

Porter, D.L., C.E.Lahm and R.G.Pahl (1990). Fuel Constituent Redistribution During the Early Stages of U-Pu-Zr Irradiation. *Metallurgical Transactions A*, **21A**, 1871.

Pugh, S.F. (1961). Swelling in Alpha Uranium Due to Irradiation. *The Metal Plutonium*, University of Chicago Press, Chap. XXXI.

Rhodes, E.A., T.H. Bauer, G.S. Stanford, J.P. Regis and C.E. Dickerman (1992). Fuel Motion in Over-Power Tests of Metallic Integral Fast Reactor Fuel. *Nuclear Technology* **98**, 91.

Sackett, J.I., W.K. Lehto and C.W. Solbrig (1990). The Role of EBR-II and Treat in Establishing Liquid Metal Reactor Safety. *Proceedings, LMR: A Decade of LMR Progress and Promise*, p.61, Washington, DC, 11–15 November.

Seidel, B.R. and R.E. Einziger (1977). *In-Reactor Cladding Breach of EBR-II Driver Fuel Elements*, Radiation Effects in Breeder Reactor Structural Materials, American Institute of Metallurgical Engineering, Chicago, Illinois.

Seidel, B.R., D.L. Porter, L.C. Walters and G.L. Hofman (1986a). Experience with EBR-II Driver Fuel. *Proceedings of the International Conference Reliable Fuels for Liquid Metal Reactors*, p.2-106, Tucson, Arizona, 7–11 September.

Seidel, B.R., G.L. Batté, C.E. Lahm, R.M. Fryer, J.F. Koenig and G.L. Hofman (1986b). Off-Normal Performance of EBR-II Driver Fuel. *Proceedings International Conf. Reliable Fuels for Liquid Metal Reactors*, p.6-48, Tucson, Arizona, 7–11 September.

Shewmon, P.G. (1958). *The Redistribution of a Second Phase During Annealing in a Temperature Gradient.* American Institute of Metallurgical Engineering. Vol. 212, 642.

Till, C.E. and Y.I. Chang(1988). The Integral Fast Reactor. *Advances in Nuclear Science and Technology 20,* 127.

Tracy, D.B., S.P. Henslee, N.E. Dodds and K.J. Longua (1989). Improvements in the Fabrication of Metallic Fuels. *Transactions of the American Nuclear Society 60*, 314.

Tsai, H. (1990). Fuel/Cladding Compatibility in Irradiated Metallic Fuel Pins at Elevated Temperatures. *International Fast Reactor Safety Meeting II*, p.257, Snowbird, Utah, 12–16 August.

Tsai, H. (1991). Behavior of Low-Burnup Metallic Fuels for the Integral Fast Reactor at Elevated Temperatures in Ex-Reactor Tests. *Conference on Fast Reactors and Related Fuel Cycles III*, 1.18-1, Kyoto, Japan, 13 October.

Van Loo, F.J.J., J.A. Van Beak, C.F. Bastin and R. Metselaar (1984). *The Role of Thermodynamics and Kinetics in Multiphase Ternary Diffusion*, Institute fur Metallphysik, Universitat Gottingen, Germany American Institute of Metallurgical Engineering, Detroit, Michigan.

Walter, C.M., N.J. Olson and G.L. Hofman (1973). EBR-II Driver Fuel Qualification and Performance. *Nuclear Metallurgy* **19**, 181.

Walter, C.M., G.H. Golden and N.J. Olson (1975). *U-Pu-Zr Metal Alloy: A Potential Fuel for LMFBRs*, Argonne National Laboratory Report ANL-76-28.

Walters, L.C., B.R. Seidel and J.H. Kittel (1984). Performance of Metallic Fuels and Blankets in Liquid-Metal Fast Breeder Reactors. *Nuclear Technology* **65**, 179.

Zegler, S.T. and C.M. Walter (1967). Compatibility Between Metallic U-Pu-Base Fuels and Potential Cladding Materials. *American Institute of Metallurgical Engineering Symposium on Plutonium Fuels Technology 13*, 335, Scottsdale, Arizona, October.